

PSU-IRL-SCI-420

Classification Numbers 1.2, 1.9.2, 3.2.2



THE PENNSYLVANIA
STATE UNIVERSITY

IONOSPHERIC RESEARCH

Scientific Report 420

PROPERTIES OF WATER VAPOR RELEVANT TO ITS MEASUREMENT IN THE STRATOSPHERE AND MESOSPHERE

by

Richard L. Longbothum

January 23, 1974

*The research reported in this document has been supported by
The National Aeronautics and Space Administration under Con-
tract No. NGL-39-009-003 and The National Science Foundation
under Contract No. GA-33446X.*

IONOSPHERE RESEARCH LABORATORY



University Park, Pennsylvania

Security Classification

DOCUMENT CONTROL DATA - R & D

(Security classification of title, body of abstract and indexing annotation must be entered when the overall report is classified)

1. ORIGINATING ACTIVITY (Corporate author)		2a. REPORT SECURITY CLASSIFICATION	
The Ionosphere Research Laboratory		2b. GROUP	
3. REPORT TITLE			
Properties of Water Vapor Relevant to Its Measurement in the Stratosphere and Mesosphere			
4. DESCRIPTIVE NOTES (Type of report and, inclusive dates)			
Scientific Report			
5. AUTHOR(S) (First name, middle initial, last name)			
Richard L. Longbothum			
6. REPORT DATE		7a. TOTAL NO. OF PAGES	7b. NO. OF REFS
January 23, 1974		116	
8a. CONTRACT OR GRANT NO.		9a. ORIGINATOR'S REPORT NUMBER(S)	
NGL-39-009-003		PSU-IRL-SCI-420	
b. PROJECT NO.		9b. OTHER REPORT NO(S) (Any other numbers that may be assigned this report)	
c.			
d.			
10. DISTRIBUTION STATEMENT			
Supporting Agencies			
11. SUPPLEMENTARY NOTES		12. SPONSORING MILITARY ACTIVITY	
		The National Aeronautics and Space Administration The National Science Foundation	
13. ABSTRACT			
<p>A detailed study of the literature on the concentrations of water vapor in the stratosphere and mesosphere is given. It is estimated that the concentrations in these regions lie in the range from 0.1 ppm to 10 ppm.</p> <p>A survey was made of the scattering and radiative transfer properties of water vapor and the background constituents to determine the physical properties of importance to measurements of concentrations. It was determined that absorption and emission properties provide significant increases in sensitivity compared with the various scattering phenomena considered. Microwave absorption in the region of 22 GHz and 183 GHz and infrared absorption in the vibrational-rotational band systems seem to be the most attractive techniques. Various experimental configurations are analyzed and compared.</p>			

PSU-IRL-SCI-420

Classification Numbers 1.2, 1.9.2, 3.2.2

Scientific Report 420

Properties of Water Vapor Relative to Its
Measurements in the Stratosphere and Mesosphere

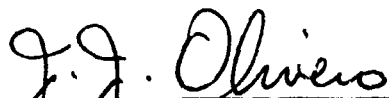
by

Richard L. Longbothum

January 23, 1974

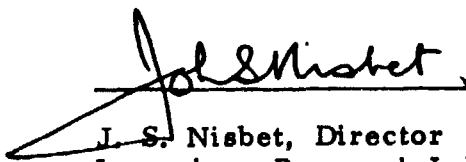
The research reported in this document has been supported by The National Aeronautics and Space Administration under Grant No. NGL 39-009-003 and The National Science Foundation under Grant No. GA 33446 X.

Submitted by:



J. J. Olivero, Assistant Professor of
Meteorology
Project Supervisor

Approved by:



J. S. Nisbet, Director
Ionosphere Research Laboratory

Ionosphere Research Laboratory
The Pennsylvania State University
University Park, Pennsylvania 16802

ACKNOWLEDGEMENTS

The author is grateful for helpful discussion with Dr. John Olivero, Dr. J. R. Mentzer, and Dr. L. C. Hale of the Ionosphere Research Laboratory and Dr. Paul Swanson of The Department of Astronomy. The research was supported by The National Aeronautics and Space Administration under Grant No. NGL 39-009-003 and The National Science Foundation under Grant No. GA 33446 X.

TABLE OF CONTENTS

	Page
ACKNOWLEDGEMENTS	ii
LIST OF FIGURES	v
ABSTRACT	vi
I. INTRODUCTION	1
II. CONSTITUENTS OF THE ATMOSPHERE	4
2.1 General	4
2.2 Water Vapor Content	6
III. ATMOSPHERIC RADIATION PROCESSES	11
3.1 General	11
3.2 Emission and Absorption	14
3.3 Raman Emission	25
3.4 Rayleigh and Mie Scattering	29
3.5 Refractive Index	36
3.6 Reflection	41
IV. MICROWAVE ABSORPTION	44
4.1 General	44
4.2 Water Vapor Absorption	56
4.3 Oxygen Absorption	60
V. INFRARED ABSORPTION.	64
5.1 General	64
5.2 The Elsasser Model of an Absorption Band.	65
5.3 The Goody Model of an Absorption Band	68
VI. METHOD OF DETECTION	72
6.1 General	72

	Page
6.2 Resonant Absorption	77
6.2.1 Passive Configuration	77
6.2.1.1 Ground Based Observations .	78
6.2.1.2 Observations from Above the Surface	79
6.2.1.3 Satellite Occultation	80
6.2.2 Active Configuration	84
6.2.2.1 Ground Based Observations .	85
6.2.2.2 Observations from Above the Surface	85
6.3 Resonant Emission	86
6.3.1 Passive Configuration	86
6.3.1.1 Ground Based Observations .	87
6.3.1.2 Observations from Above the Surface	89
6.3.2 Active Configuration	90
6.3.2.1 Ground Based Measurements	91
6.4 Raman Scatter	92
6.4.1 Ground Based Observations	93
VII. SUMMARY AND DISCUSSION	95
APPENDIX A The Water Vapor Molecule	99
APPENDIX B Molecular Oxygen	103
APPENDIX C Mie Scatter Approximation	105
APPENDIX D Derivation of Elsasser's Infrared Absorption Model	107

LIST OF FIGURES

Figure	Page
1. Atmospheric Composition between 20 and 120 km Altitude	5
2. Water Vapor Mixing Ratio Profile from 0 to 32 km Altitude	8
3. Theoretical Models of Water Vapor Density	10
4. Volume Backscatter Coefficients for a Clear Standard Atmosphere	35
5. Rotational frequencies and Absorption Coefficients of Atmospheric Gases between 10 GHz and 100 GHz	45
6. Total Attenuation for One Way Transmission through the Atmosphere.	47
7. Attenuation per Kilometer for Horizontal Propagation.	48
8. Calculated Water Vapor Absorption for 7.5 g/m^3 with $\Delta\nu/c = 0.1$	50
9. Measured Atmospheric Absorption Spectra.	51
10. Occultation Experiment	82
11. Zenith Attenuation Versus Frequency.	96
12. Line Frequencies of Several Atmospheric Gases.	97
13. Water Vapor Molecule.	102

ABSTRACT

A detailed study of the literature on the concentrations of water vapor in the stratosphere and mesosphere is given. It is estimated that the concentrations in these regions lie in the range from 0.1 ppm to 10 ppm.

A survey was made of the scattering and radiative transfer properties of water vapor and the background constituents to determine the physical properties of importance to measurements of concentrations. It was determined that absorption and emission properties provide significant increases in sensitivity compared with the various scattering phenomena considered. Microwave absorption in the region of 22 GHz and 183 GHz and infrared absorption in the vibrational-rotational band systems seem to be the most attractive techniques. Various experimental configurations are analyzed and compared.

CHAPTER I

INTRODUCTION

The problem of how much water vapor exists in the stratosphere and above is one that has received attention for a considerable number of years but which has still not yet been fully answered.

The amount of water vapor in the upper atmosphere is a critical problem since it plays an important part in the chemistry and heat budget of the atmosphere. Water vapor may be responsible for destroying ozone and contributes to the escape of hydrogen through photodissociation. It is thought to be responsible for hydrated ions, OH airglow emissions, and may control ionization loss processes as high as 80 km. Water vapor is involved in O - H - N photochemistry in the mesosphere, and there is a strong possibility that the existence of noctilucent clouds is dependent on the amount of water vapor present near the 80 km level.

Mastenbrook (1971) reported the observed increase in mixing ratios of water vapor from two parts per million to three parts per million through the six year period from 1964 to 1969. This increase was observed at all pressure levels from 15 km to 21 km.

For these reasons and more, it is important to develop a method of detecting and measuring the concentration of water vapor in the atmosphere from the surface of the earth up to about 100 km where the H₂O mixing ratio is probably seriously reduced through dissociation by solar ultraviolet radiation.

At the present time, the highest experimental measurements of water vapor have been about 32 km. Thus, there is a large height range, 30 km to 90 km, where little is known about its concentration. This

report discusses various detection techniques that could be used for observing water vapor and making measurements. In order to set the background, Chapter I of the report discusses the present knowledge about the concentration of water vapor in the atmosphere, both experimental and theoretical. Also, the attenuation of radiation by water vapor is discussed in order to understand the interaction of electromagnetic radiation with the water vapor molecule (which is the basis of several of the detection techniques considered).

In Chapter II the concentration of the atmospheric constituents is discussed, and all that is known currently about the water vapor distributions is reviewed. The theory of the various physical radiation processes present in the atmosphere is discussed in Chapter III with a physical description of the radiative transfer of energy through an atmospheric volume, and the refractive index of the atmosphere is related to the atmospheric properties of pressure, temperature, density of constituents, etc.

Chapter IV then follows with special attention given to the microwave frequency range. The various absorption coefficients for water vapor and oxygen molecules valid in this range are presented.

The theory of infrared absorption is presented in Chapter V with the band models of Elsasser and Goody being discussed.

In Chapter VI the various methods of radiometry which can be used to detect and measure the water vapor concentrations are discussed in terms of their basic strengths and weaknesses. The basic configurations in which the methods can be used are also discussed. Some of the factors which are inherent in the atmosphere and that complicate the various detection and measurement processes are considered.

In the last chapter an attempt is made to draw some conclusions about the various methods of detection, the optimum frequency ranges of operation, etc. The reasons for the selections are presented although at this point no method seems to be outstanding overall. Each method has its weak and strong points.

The physical and molecular properties of water vapor are discussed in Appendix A so that some understanding of the behavior of the interaction between the molecule and the incident electromagnetic field can be obtained.

In Appendix B the properties of the oxygen molecule are discussed since non-resonant absorption by oxygen interferes with the water vapor lines in the otherwise relatively clean region of the microwave spectrum.

In Appendix C, series approximations to the Mie scattering coefficient are presented.

Finally, in Appendix D, the derivation of Elsasser's infrared absorption model is presented.

CHAPTER II

CONSTITUENTS OF THE ATMOSPHERE

2.1 General

The major constituents of the atmosphere up to about 120 km are molecular nitrogen and molecular oxygen. Also present are small amounts of argon, carbon dioxide, water vapor, etc. (see Figure 1). Molecular oxygen is dissociated by solar ultraviolet radiation in the mesosphere and thermosphere. The concentration of O_2 , thus, decreases while the concentration of atomic oxygen (O) increases with increasing altitude. At about 120 km the concentration of O is greater than that of O_2 ; at 500 km practically no O_2 remains. Molecular nitrogen is much more difficult to dissociate and even at 500 km the concentration of atomic nitrogen (N) is very small. Above 100 km the effects of diffusive separation do become important, and thus, the lighter gases tend to predominate in the upper regions compared with the heavier gases in the lower regions. As a result of molecular diffusion, helium and hydrogen are the principal constituents in the extreme upper atmosphere.

The concentration of carbon dioxide in the atmosphere is approximately constant at least up to 80 km. The maximum ozone density is usually found between 20 and 30 km. The number density of ozone at its maximum is of the order of $5 \times 10^{12} \text{ cm}^{-3}$. As this means there is only one ozone molecule to about 10^5 oxygen and nitrogen molecules, we can expect that ozone will not play a significant part in any non-resonant scattering experiments. In the case of water vapor, experimental information concerning the variation with height above the tropopause is poor.

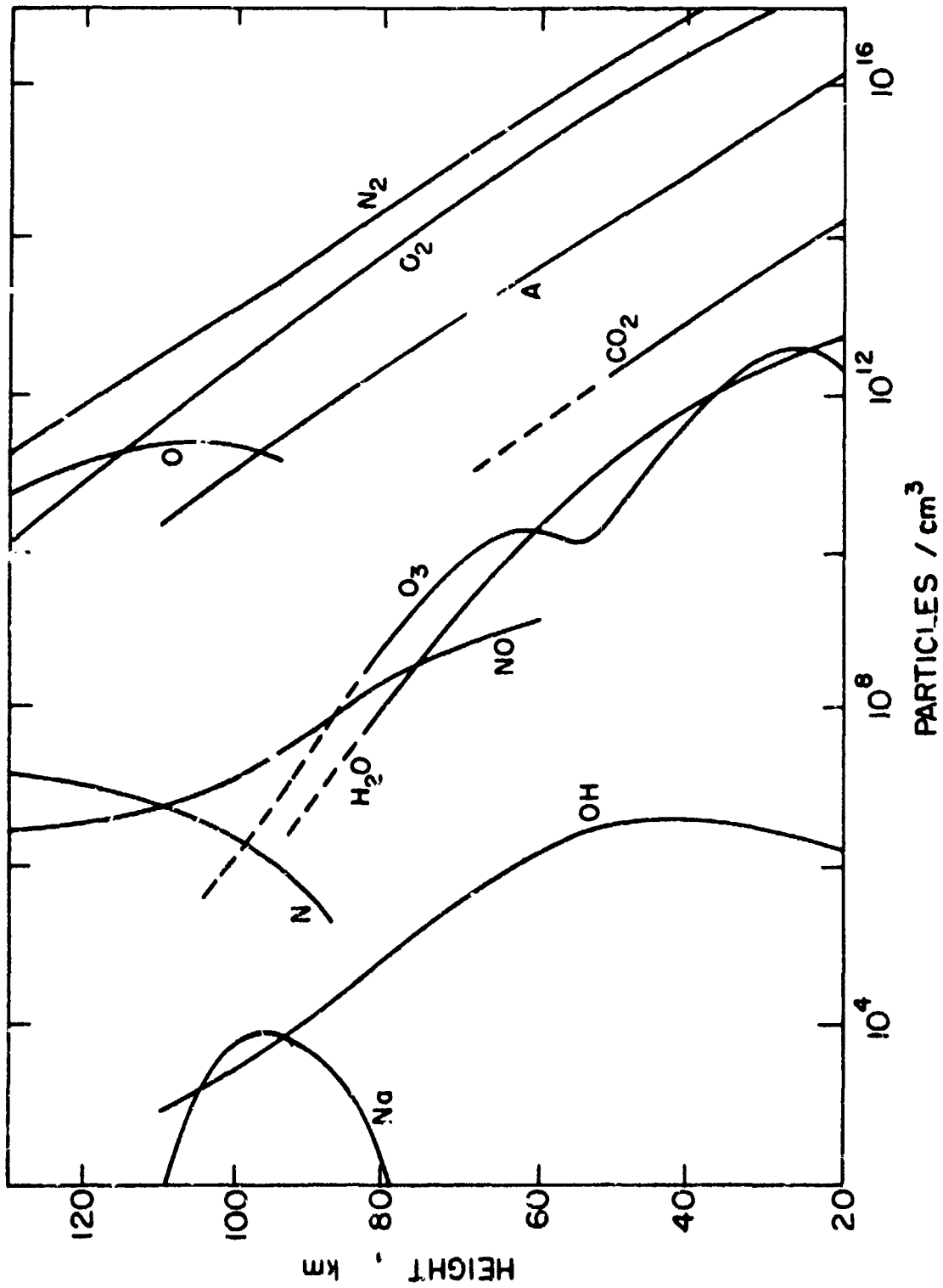


Figure 1: Atmospheric composition between 20 and 120 km altitude (Kent, G. S. and Wright, R. W. H., 1970)

2.2 Water Vapor Content

The first measurements of stratospheric water vapor were made by the British in 1953 using a manually operated frost point hygrometer on an aircraft (Mastenbrook, 1968). The frost point hygrometer when used as a sounding instrument provides a vertical distribution of water vapor in terms of the frost point temperature. From the known relation of frost point temperature and partial pressure of water vapor formulated by Goff and Gratch (1946), the concentration of water vapor is determined using the perfect gas law

$$p_{\text{H}_2\text{O}} = n_{\text{H}_2\text{O}}KT \quad (2.1)$$

or

$$p_{\text{H}_2\text{O}} = \rho_{\text{H}_2\text{O}} \frac{RT}{m_{\text{H}_2\text{O}}} \quad (2.2)$$

where $\rho_{\text{H}_2\text{O}}$ is water vapor density and $m_{\text{H}_2\text{O}}$ is the molecular weight of water vapor. When $p_{\text{H}_2\text{O}}$, the partial pressure of H_2O , and $n_{\text{H}_2\text{O}}$, the concentration of H_2O , are the saturated values, the value for T is the frost point temperature (or dew point temperature where appropriate).

The British observed in their measurements that humidity decreased rapidly with height above the tropopause and mixing ratios¹ as low as 2×10^{-6} (two parts per million) were found (Mastenbrook, 1968). Using the same technique, Mastenbrook obtained a median vertical distribution of water vapor for the lower stratosphere to a height of 28 km which approximates a constant mixing ratio within the range of

¹The mixing ratio is the ratio of the mass of water vapor present to the mass of dry air present in a unit volume.

2×10^{-6} to 3×10^{-6} (two to three parts per million). He found that the vertical gradient in the lower stratosphere reversed seasonally. The gradient is negative in the late winter and spring and positive in the late summer and fall. The change of gradient is attributed to the seasonal change of moisture in the low stratosphere (Mastenbrook, 1968).

A few years ago, Sissenwine (1968) reported that the British consider the mixing ratio to be about two parts per million at the 16 km level. In this case the water vapor density tends to become monotonically lower as the atmospheric density falls off with altitude. Then since frost point (and dew point) have a one to one relationship with absolute humidity (water vapor density), they would also have a parallel decrease with altitude. Sissenwine (1968) conducted his own investigation using a balloon at 32 km and after solving the water vapor outgassing problem, concluded that his findings reinforced the British findings of a mass mixing ratio of 0.002 gm/kg at the 16 km level (100 mb) which was the maximum altitude of the original British aircraft data. His results ranged from 1 to 10 parts per million. These results also showed that above this level the water vapor density increased to a relative maximum at 25 km (from a humidity minimum above the tropopause at about 15 km) (see Figure 2).

Keneshea, et al. (1972) presented a density profile of water vapor which was calculated theoretically from 40 to 150 km and for 30°N equinox and 60°N winter using a photochemical model. Sechrist (1972) collected theoretical water vapor profiles of Shimazaki and Laird (1970), Anderson (1971), Bowman, Thomas, and Geisler (1970). Shimazaki and Laird and Bowman, Thomas, and Geisler used photochemical transport models while Anderson deduced water vapor

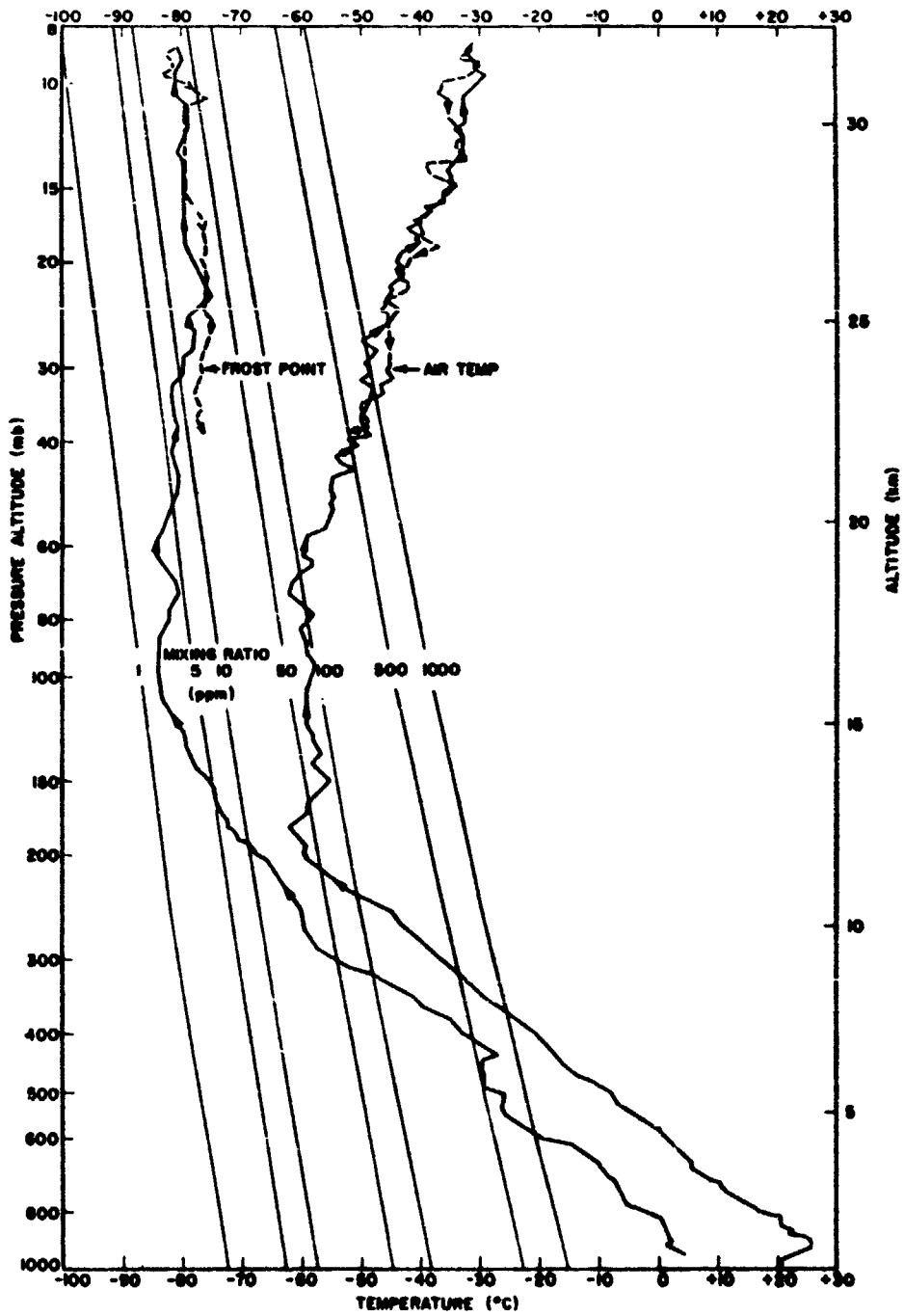


Figure 2: Water vapor mixing ratio profile from 0 to 32 km altitude (Sissenwine, N. et al, 1968; reprinted by permission of the American Meteorological Society)

concentrations inferred from rocket borne fluorescent scattering observations (see Figure 3).

In one of the more recent papers, Mastenbrook (1971) published the results of a six year study in which monthly samples were taken over Washington, D. C. and a steady increase of water vapor mixing ratio from 2×10^{-6} to 3×10^{-6} has been observed. The increase was observed at all pressure levels from 100 mb (15 km) to 50 mb (21 km). This increase suggests that stratospheric water vapor may possibly be an indication of climatic variations occurring at lower levels.

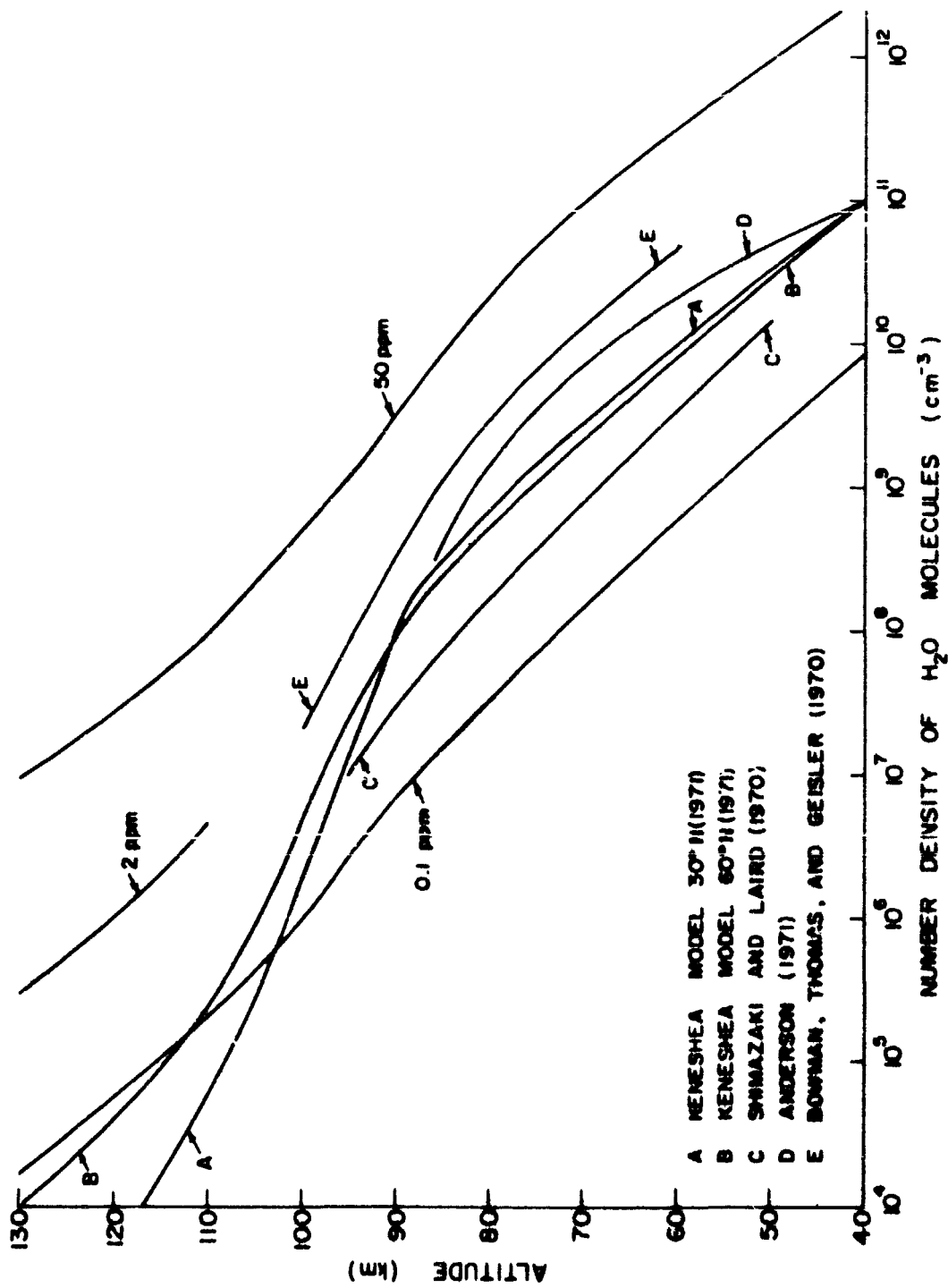


Figure 2: Theoretical models of water vapor density

CHAPTER III
ATMOSPHERIC RADIATION PROCESSES

3.1 General

The atmosphere is a turbid medium composed of atomic and molecular gases and aerosols which are solid or liquid (or a combination thereof) particles of different sizes suspended in the air.

Electromagnetic energy incident upon a volume of this gas-particle mixture is both scattered and absorbed in accordance with Beer's law which governs the extinction of energy by the atmosphere.

$$\frac{dI}{I} = - \sigma dz \quad (3.1)$$

where in general

$$\sigma = K_s + K_a + K_r \quad (3.2)$$

K_s = the scattering coefficient

K_a = the absorption coefficient

K_r = the reflection coefficient

In addition absorption and emission of radiation occurs in the atmosphere entirely independently of external sources of electromagnetic radiation. The latter is caused by thermal (black body) radiation resulting from the collisions between molecules and particles undergoing thermodynamic processes. Thermal or black body radiation has a continuous spectrum which is described by the Planck function. Thus the total change of intensity of radiation in passage through an atmospheric region governed by an equation of the form

$$\frac{dI}{dz} = -\sigma (I - E) \quad (3.3)$$

where E is the source function related to the thermal radiation intensity given by Planck's function

$$E \propto \frac{2h\nu^3}{c^2} \frac{1}{e^{\frac{h\nu}{kT}} - 1} \quad (3.4)$$

The physical picture one may draw from this equation is that a wave of intensity I incident upon an atmospheric volume in thermodynamic equilibrium is, in general, scattered in directions other than that of the direction of propagation (although some forward scatter will be in the direction of the wave), reflected by discontinuities in the gas mixture, and absorbed. Absorption occurs whenever the electromagnetic energy of the wave raises the molecules to excited states, and then before the molecules can reradiate, collisions occur during which non-radiating transitions (deactivation) take place. Emission occurs both continuously from thermal processes and discretely from molecular transitions triggered by the incident wave. Thus, the intensity of radiation leaving the volume (transmitted) is that portion of the wave that has not been scattered, reflected, or absorbed, plus that amount which has been forward scattered and emitted by excited molecules in the reference direction.

In order to avoid confusion, the processes should be defined on a precise basis. For this study emission is defined as the radiation process in which there is a decrease in internal energy of the molecule. Actually, there are two types of emission. When the transition to a lower state takes place in one step so that the emitted quantum has the same frequency as the absorbed quantum, coherent emission occurs,

which is also known as resonant scattering. The other type is called fluorescent or incoherent emission. In this case the molecule returns to the ground state through a cascade process among intermediate levels. When frequencies are emitted lower than that of the absorbed quantum, these lines are called Stoke's lines and the process is known as Stoke's fluorescence. When higher frequencies than that of the absorbed quantum are emitted, the lines are called anti-Stoke's lines and the process is called anti-Stoke's fluorescence. Anti-Stoke's lines are weaker than Stoke's lines by a factor of 10^{-3} because the energy in balance must be made up by translational kinetic energy (K. E.).

A process related to fluorescent emission is that of Raman scattering. Raman scatter differs from fluorescent emission in that for fluorescence, the incident photon is completely absorbed and the molecule is thereby raised to an excited state, whereas in Raman scattering, the photon as a whole is never absorbed, but rather simply perturbs the molecule and induces it to undergo a vibrational or rotational transition and that portion of the photon energy remaining becomes the scattered radiation.

In addition to the process of emission is that of absorption in which the energy is transferred to the molecule to raise it to a higher state. However, before the molecule can reradiate, the energy may be removed in the form of kinetic energy by collisions. All of these processes involve a change in the internal energy of the molecule and must be described by quantum mechanics in terms of probabilities called Einstein coefficients.

In addition there exist electromagnetic scattering mechanisms such as elastic scattering and reflection. Scattering can be defined as

an elastic process in which there is no internal energy change of the molecules. The process does not emit radiation, but only results from a perturbation of the wavefront by the scattering particle. The perturbation then acts as a secondary wave propagating out from the particle or molecule. This process is described by classical electromagnetic field theory.

The same is true for the process of reflection. The main difference between this process and that of scattering is that scattering occurs from individual particles where $l \gg \lambda$ (l being the distance between particles and is proportional to n^{-3} , and λ is the wave length of the incident wave). However, for the case of reflection, $l \ll \lambda$ so that a layer of particles creates a fluctuation or discontinuity in refractive index, which then causes a reflection of the wave.

3.2 Emission and Absorption

Molecules can exist in either the ground state or excited states. Though they are neutral, they can possess both electric and magnetic dipoles or higher order multipoles. The mechanism of energy transfer between matter and radiation is most commonly by coupling between the electric component of the radiation field and the electric dipole of the molecule or between the molecular magnetic dipole and the magnetic field component. This energy transfer may occur over a broad band of frequencies (non-resonant absorption) or it may be a sharp line resonance transfer (resonant absorption). If, as a result of the interaction, the radiation field loses energy to the molecule, absorption occurs. Conversely, if the radiation field gains energy from the molecule, emission occurs.

There are three basic types of radiation field molecule interaction: absorption, induced or stimulated emission, and spontaneous emission. In absorption a photon is absorbed by the molecule which is then raised to a state of higher energy. Induced emission is the reverse process, where the molecule (already in an excited state), under the influence of the applied electromagnetic field, emits a photon at the frequency of the applied field and drops to a lower internal energy level. In spontaneous emission, a molecule in an excited energy state, even though it is undisturbed by an applied field, emits a photon at the characteristic frequency given by the Bohr frequency condition ($h\nu_{ij} = E_i - E_j$) and drops to a lower energy state. The processes of absorption and induced emission are coherent processes since the same incident wave acts on all the molecules, whereas the process of spontaneous emission is usually an incoherent process since it is random in nature. Thus, the resulting spontaneous emission signal power is much less than that obtainable in a coherent absorption or emission process. The rate of spontaneous emission occurring from an upper level E_i to a lower level E_j depends only on the number of molecules in the upper level, N_i . The rate of stimulated emission and absorption depends on the populations N_i and N_j . These types of interaction were dealt with by Einstein. His B coefficient gives the probability for either absorption or induced emission, and his A coefficient gives the spontaneous emission probability (Barrett, 1958).

Several life times are important for resonance absorption and emission. The excited molecules reach rotational equilibrium before they decay back to the ground state because of the fast rotational relaxation time of the order of 10^{-9} seconds at standard temperature

and pressure (STP). The non-radiative vibrational relaxation time is much longer, and is approximately 10^{-4} to 10^{-6} seconds at atmospheric pressure, depending on the molecule. The spontaneous radiation decay time is even longer being about 10^{-1} to 10^{-2} or more seconds for metastable states. Since the non-radiative vibrational decay time is much faster (at STP) than the radiative decay time, the resonance emission efficiency is reduced by about the ratio between the two decay times (Kildal, et al., 1971).

To discuss the process of absorption and induced emission, it is helpful to consider a molecular gas having two energy levels E_1 and E_0 , having n_1 and n_0 molecules per cubic centimeter in the upper and lower energy levels, respectively. Let ν_0 be the resonant frequency defined by these levels, where $h\nu_0 = E_1 - E_0$. Then radiation incident on this gas in a range of frequencies close to ν_0 will be absorbed by molecules initially in the lower state. The incident radiation will supply energy $h\nu_0$ necessary to cause a molecule to make a transition from the lower to the upper energy level and a photon of energy $h\nu_0$ will be removed from the radiation field. Likewise, the radiation can induce or stimulate transitions in the reverse direction, from the upper to the lower energy level, and this stimulated emission will add a photon of energy $h\nu_0$ to the radiation field. The net absorption by the gas is the difference between the number of absorptions and number of emissions. If a molecule in the lower state is capable of absorbing energy of frequency ν , the probability of absorption per molecule per second is $B_{01} \rho(\nu)$ where $\rho(\nu) d\nu$ is the energy density of the incident radiation in the frequency range between ν and $\nu + d\nu$ and B_{01} is the Einstein B coefficient for absorption. The number of

molecules per cubic centimeter capable of absorbing energy at frequency ν can be written as $n_0 f(\nu)$ where $f(\nu)$ is the fraction of molecules able to absorb at frequency ν . The fraction $f(\nu)$ will depend on the molecular velocities in the case of a Doppler broadened line, on the width of the energy levels in the case of a line broadened by stimulated emission, and on pressure in the case of a line broadened by collisions. In either case, $f(\nu)$, the line shape function, is subject to the condition

$$\int_0^{\infty} f(\nu) d\nu = 1 \quad (3.6)$$

Thus the number of absorptions per cubic centimeter per second at frequency ν is

$$n_0 f(\nu) B_{01} \rho(\nu) \quad (3.7)$$

Similarly, the number of induced or stimulated emissions per cubic centimeter per second is

$$n_1 f(\nu) B_{10} \rho(\nu) \quad (3.8)$$

where B_{10} is the Einstein B coefficient for induced emission and is related to B_{01} by the relation (Barrett, 1958)

$$g_0 B_{01} = g_1 B_{10} \quad (3.9)$$

The numbers g_0 , g_1 are statistical weights of order unity and are pure numbers. They represent the number of sublevels which compose the energy levels 0 and 1, respectively (Barrett, 1958).

The net number of absorptions is

$$\begin{aligned}
 & n_0 f(\nu) B_{01} \rho(\nu) - n_1 f(\nu) B_{10} \rho(\nu) \\
 &= n_0 f(\nu) B_{01} \rho(\nu) - n_1 f(\nu) \frac{g_0}{g_1} B_{01} \rho(\nu) \quad (3.10) \\
 &= n_0 f(\nu) B_{01} \rho(\nu) \left[1 - \frac{n_1 g_0}{n_0 g_1} \right]
 \end{aligned}$$

Before continuing with the case of absorption and induced emission, it is important to discuss the case of spontaneous emission as this process has been neglected in the net absorption equation

As has been mentioned, the line width can be broadened by spontaneous emission or natural broadening. This is because one or both of the energy (states) of the transition may have a short lifetime. Molecules in such a level or state will not remain in that state if they can "make a transition by photon emission". If a molecule is assumed to be in a particular state at time $t = 0$, the probability of finding the molecule in that state at time t is the Einstein A coefficient and is given by quantum mechanics as

$$A = \frac{64 \pi^4 \nu^3 |\mu|^2}{3hc^3} \quad (3.11)$$

where μ is the electric dipole moment. By Fourier analysis of radiation from an oscillator whose amplitude is decaying with time according to $e^{-\frac{At}{2}}$ (the energy is decaying at the rate e^{-At}), one can obtain a frequency spectrum of the form (Barrett, 1958)

$$I(\nu) = \frac{I_0}{(\nu - \nu_0)^2 + (A/4\pi)^2} \quad (3.12)$$

or the radiation has a line width $A/2\pi$. The other forms of line broadening, pressure broadening and Doppler broadening, will be discussed later in this section.

Note that A depends on the frequency of the incident wave ν in a cubic fashion. Thus, A is larger for optical frequencies than it is for radio frequencies.

The mechanism of spontaneous emission is the principal cause of the continuous emission spectrum generated by the thermal processes within the atmospheric gas. The net number of emissions is given by

$$n_1 f(\nu) A + n_1 f(\nu) B_{10} \rho(\nu) = n_1 f(\nu) [A + B_{10} \rho(\nu)] \quad (3.13)$$

The net number of absorptions is given by

$$n_0 f(\nu) B_{01} \rho(\nu) \quad (3.14)$$

At (thermal) equilibrium, the sum of the emissions is equal to that of the absorptions

$$n_1 f(\nu) [A + B_{10} \rho(\nu)] = n_0 f(\nu) B_{01} \rho(\nu) \quad (3.15)$$

Then using

$$\frac{n_1}{n_0} = \frac{g_1}{g_0} e^{-\frac{h\nu_0}{kT}} \quad (3.16)$$

One may obtain

$$\rho(\nu) \left[B_{01} - B_{10} \frac{g_1}{g_0} e^{-\frac{h\nu_0}{kT}} \right] = \frac{g_1}{g_0} A e^{-\frac{h\nu_0}{kT}} \quad (3.17)$$

and it can be shown (Barrett, 1958) that

$$g_0 B_{01} = g_1 B_{10} \quad (3.9)$$

so that

$$B_{01} \left[1 - e^{-\frac{h\nu_0}{kT}} \right] \rho(\nu) = \frac{g_1}{g_0} e^{-\frac{h\nu_0}{kT}} A \quad (3.18)$$

or the radiation density $\rho(\nu)$ is

$$\rho(\nu) = \frac{g_1/g_0 A}{B_{01} \left(e^{\frac{h\nu_0}{kT}} - 1 \right)} \quad (3.19)$$

but

$$A = \frac{8\pi \nu^3 h}{c^3} B_{01} \quad (3.20)$$

and if $g_1 = g_0$

$$\rho(\nu) = \frac{8\pi \nu^3 h}{c^3} \frac{1}{e^{\frac{h\nu_0}{kT}} - 1} \quad (3.21)$$

This is the Planck Blackbody formula which describes the continuous spectrum from thermal radiation. Returning to the discussion of absorption and induced emission, the relative number of molecules in levels 1 and 0 can be related by the Boltzmann distribution for a medium in local thermodynamic equilibrium (collisions dominate radiative transfer in determining populations).

$$\frac{n_1}{n_0} = \frac{g_1}{g_0} e^{-\frac{(E_1 - E_0)}{kT}} = \frac{g_1}{g_0} e^{-\frac{h\nu_0}{kT}} \quad (3.22)$$

This can be written for radio frequencies up through the microwave range where $h\nu_0 \ll kT$ as

$$\frac{n_1}{n_0} = \frac{g_1}{g_0} \left[1 - \frac{h\nu_0}{kT} \right] \quad (3.23)$$

The change in energy density $d\rho(\nu)d\nu$ per unit path length $d\ell$ through the gas is $\frac{h\nu}{c}$ times the net absorptions per cm^3 per second or (Barrett, 1958)

$$\frac{d\rho(\nu)d\nu}{d\ell} = \frac{n_0 f(\nu) B_{01} \rho(\nu) h^2 \nu^2}{ckT} \quad (3.24)$$

The absorption coefficient $K_a(\nu)$ (the fractional change in energy density per unit length) becomes

$$K_a(\nu) = \frac{d\rho(\nu)d\nu}{\rho(\nu)d\ell} = \frac{n_0 f(\nu) B_{01} h^2 \nu^2}{ckT} \quad (3.25)$$

The Einstein B coefficient to be inserted into the above formulation is, from quantum mechanics,

$$B_{01} = \frac{8\pi^3 |\mu|^2}{3h^2} \quad (3.26)$$

In most atmospheric attenuation work, the total absorption is given in terms of opacity or optical depth $\tau(\nu)$ where

$$\tau(\nu) = \int K_a(\nu) d\ell \quad (3.27)$$

It can be shown that for N_0 molecules in level 0 contained in a column along the line of sight of one cm^2 cross section where

$$N_0 = \int n_0 d\ell \quad (3.28)$$

that

$$\tau(\nu) = \frac{8\pi^3 N_0 \nu^2 |\mu|^2}{3ckT} f(\nu) \quad (3.29)$$

For a line broadened only by spontaneous emission, the line shape $f(\nu)$ is (Barrett, 1958)

$$f(\nu) = \frac{1}{\pi} \frac{\Delta\nu}{(\nu - \nu_0)^2 + (\Delta\nu)^2} \quad (3.30)$$

which is proportional to Equation (3.12). Using this expression for the opacity of the gas, one can describe how the presence of the molecular gas will affect the intensity of radiation received by a radiometer (Barrett, 1958).

Although the preceding theory considered only two states, more than two possible energy states exist for all molecules. However, it is not possible to cause transitions between every pair of internal energy states; restrictions are imposed on what pairs of states may be coupled by both radiative and non-radiative transitions. These restrictions are known as selection rules and are expressed in terms of allowed changes in the quantum numbers specifying the internal states. In the theory of interaction of an atom or molecule with electromagnetic radiation, the effectiveness of radiation on the atom or molecule is given by the dipole matrix element μ_{ij} which is obtained quantum mechanically. This matrix element depends on the initial and final states of the transition and like its classical counterpart, can be classified as either electric or magnetic. As can be seen from either Einstein's A or B coefficients, when a transition takes place, the intensity of emitted radiation is proportional to the square of the matrix element and this provides the key to the selection rules. When the matrix elements are calculated quantum mechanically, many cases turn out to be zero and it becomes possible to predict quite generally which combinations of initial and final state quantum numbers will give results different from zero.

One important property of these transitions is that the electric dipole moment is of the order of 100 times the magnetic dipole moment, and since the intensity of emitted radiation varies as the square of the

dipole matrix element, electric dipole transitions are some 10^4 times as intense as magnetic dipole transitions. Thus, the concentration of molecules possessing electric dipole transitions can be much smaller than those of magnetic dipoles and still be detectable.

There are three main sources of the broadening of the atmospheric spectral lines. Pressure or collisional broadening exists because of collisions and longer range interactions between the radiating molecule and other molecules. In this form of broadening, the atoms or molecules are assumed to have a definite collision radius and each radiating molecule periodically suffers a sudden disruption of the radiation mechanism. The collision either stops the radiating process or changes the phase by an arbitrary amount. Fourier integral analysis of the wave train yields the observed frequency distribution of spectral intensity. The result is the dispersion line form (Foley, 1946)

$$I(\omega) = \frac{c}{\pi} \frac{n\pi a^2 \bar{v}}{(n\pi a^2 \bar{v})^2 + (\omega - \omega_0)^2} \quad (3.31)$$

with a half width in angular frequency units of $2n\pi a^2 \bar{v}$ where n is the number of molecules per cubic centimeter, a is the collision radius and \bar{v} is the mean velocity of the molecules. Note that this expression is similar to Equations (3.12) and (3.30).

This form of broadening is dominant in planetary or solar atmospheres. It is dominant in our atmosphere up to at least the upper stratosphere.

The next most important form of line broadening is Doppler broadening which becomes dominant where pressure broadening recedes in importance. This process results from the fact that an atom or molecule emitting or absorbing radiation is not stationary, but is

constantly in motion. For the case of molecules moving along the line of sight with velocity v , the frequency of its transition will appear shifted by an amount given by the well known Doppler formula (Barrett, 1958)

$$\nu - \nu_0 = \frac{\nu_0}{c} \cdot v \quad (3.32)$$

where ν is the observed frequency and ν_0 is the resonant frequency of the stationary molecule. The velocity is assumed to be given by the Maxwellian velocity distribution

$$f(v) = 4\pi \left(\frac{M}{2\pi kT} \right)^{3/2} v^2 \exp \left(- \frac{Mv^2}{2kT} \right) \quad (3.33)$$

where M is the mass of the molecule. For this case, the intensity distribution of emitted radiation is given by (Barrett, 1958)

$$I(\nu) = I_0 \exp \left[- \frac{M}{2kT} \left(\frac{c}{\nu_0} (\nu - \nu_0) \right)^2 \right] \quad (3.34)$$

which yields the line width as

$$\Delta\nu = 2 \frac{\nu_0}{c} \sqrt{\frac{2kT}{M} \ln 2} \quad (3.35)$$

where $\Delta\nu$ is the full width at half maximum intensity. The last important form of broadening is that of natural broadening by spontaneous emission which has already been described.

Thus far the absorption and emission processes have been general as to the frequency range. The internal energy of a molecule is normally characterized by three types of energy: 1) electronic, associated with the motion of electrons in various molecular orbits, with energy changes typical of visible radiation,*2) vibrational, due to nuclear vibrations, with energy changes typical of infrared radiation,

and 3) rotational, associated with the end over end rotation of the entire molecule, with energy changes usually typical of microwave radiation. Thus, the absorption and emission spectrum can be conveniently broken into various frequency ranges: microwave, infrared, visible, and ultraviolet. The most common ranges of interest in studying water vapor are the microwave and infrared ranges, although visible frequencies are, with the advent of high power lasers, becoming increasingly important. For this study only the microwave and infrared frequency ranges are considered.

A problem also to be considered is that in the microwave range, pressure broadening differs from that at infrared and optical frequencies because the broadening results mainly from non-adiabatic collisions (collisions which produce sufficient kinetic energy to make a transition from the ground state to an excited state as well as causing a change of phase of the oscillator). At infrared and optical frequencies there is insufficient kinetic energy available to make this transition and the collisions are adiabatic, the broadening being produced by a change in phase of the oscillator due to inter-molecular interactions during the collision, rather than a change in energy of the oscillator (Townes and Schawlow, 1955).

3.3 Raman Emission

The Raman effect is the scattering of electromagnetic radiation by matter with a change of frequency. The process is similar to Rayleigh scattering where no change in frequency occurs. The mechanism of Raman emission can be explained using a classical approach, although there are some details which must be obtained using quantum mechanics.

For an incident electromagnetic wave of frequency ν_0 , the induced dipole moment in a polar molecule may be written as (Anderson, 1971)

$$\bar{\mu} = \alpha \bar{E}_0 \cos 2\pi \nu_0 t \quad (3.36)$$

where

α is the molecular polarizability

E_0 is the amplitude of the electric field

The polarizability will vary with the configuration of the molecule, that is, be a function of the vibrational or other motion of the nuclei, so that for a given normal mode of frequency ν_m

$$\alpha = \alpha_0 + \alpha_1 \cos [2\pi \nu_m t + \beta] \quad (3.37)$$

where β is an arbitrary phase.

Thus, the dipole moment can be written as

$$\bar{\mu} = E_0 \alpha_0 \cos 2\pi \nu_0 t + E_0 \alpha_1 \cos 2\pi \nu_0 t [\cos (2\pi \nu_m t + \beta)] \quad (3.38)$$

The molecule can now be viewed as an oscillating dipole which radiates power at a rate given by

$$I = \frac{16\pi^4 \nu^4}{3c^3} |\bar{\mu}|^2 \quad (\text{Anderson, 1971}) \quad (3.39)$$

In terms of the preceding equation the expression becomes

$$I = \frac{16\pi^4 \nu^4}{3c^3} \left[\alpha_0^2 E_0^2 \cos^2 2\pi \nu_0 t + \alpha_1^2 E_0^2 \cos^2 [2\pi(\nu_0 + \nu_m)t + \beta] + \alpha_1^2 E_0^2 \cos^2 [2\pi(\nu_0 - \nu_m)t - \beta] + \text{cross terms} \right] \quad (3.40)$$

Thus, it can be seen, since the cross terms can usually be neglected, that the intensity of scattered radiation contains a term of the same frequency as the incident wave and is of the same phase. Thus, there is coherent Rayleigh scattering present at all times. The other two terms show that there will be a sum and a difference frequency radiated with different amounts of phase. The phase will be different for each scattering molecule so that the observed radiation which is the sum of that from all the scatters will be incoherent.

This form of scattering provides a unique molecular signature. However, it is the weakest of all atmospheric radiation processes considered, having cross section near that of Rayleigh scatter.

As was shown above, for an incident wave of frequency ν_0 , Raman lines occur at a series of frequencies $\nu_0 \pm \nu_1, \nu_0 \pm \nu_2, \dots$. The lower frequencies are called Stokes lines and the higher frequencies are called anti-Stokes lines. The anti-Stokes lines are normally the weaker of the two. The frequency displacement is related to the rotation-vibration spectrum of a molecule, however, selection rules differ from those operating in the infrared spectrum (where $\Delta J = \pm 1$). The Raman cross sections vary widely for the individual atmospheric components, however, they are in general less than Rayleigh cross sections. Thus, to obtain similar signal levels when using Raman scatter, some of the range capability available when using Rayleigh scatter is traded off to compensate for the smaller interaction parameters. The N_2 vibrational (vibrational-rotational) cross section is presently estimated to be about 2.0×10^{-3} of the Rayleigh scatter cross section and a similar situation exists for O_2 .

As was mentioned, the classical analysis does not yield all the answers about Raman scatter. Quantum theory explains why the anti-Stokes line is weaker. This is due to the fact that anti-Stokes lines arise only from excited molecules which are in a minority according to the Boltzmann distribution.

The intensity of Raman lines after averaging over all orientations of the molecule and where the molecule makes a transition from state m to state n (Derr, et al., 1970) is given by the following,

$$I_{mn} = \frac{2^7 \pi^5}{3^2 c^4} I_0 (\nu_0 - |\nu_{mn}|)^4 \sum_{\rho, \sigma} |(\alpha_{\rho\sigma})_{mn}|^2 \quad (3.41)$$

where ρ, σ are independently x, y, or z.

$$(\alpha_{\rho\sigma})_{mn} = \frac{1}{\hbar} \sum_r \left[\frac{(M_\rho)_{rn} (M_\sigma)_{mr}}{\nu_{rm} - \nu_0} + \frac{(M_\rho)_{mr} (M_\sigma)_{rn}}{\nu_{rn} + \nu_0} \right] \quad (3.42)$$

and

$$(M_\rho)_{mr} = \int \psi_r^* \mu_\rho \psi_m d^3r = \bar{\mu}_{mr} \quad (3.43)$$

c = speed of light

I_0 = incident plane polarized intensity of frequency ν_0

r = an intermediate state

$\bar{\mu}_{mr}$ = transition moments of the dipole moment operator $\bar{\mu}$.

There is also the process of resonant Raman scatter in which by choosing the incident radiation frequency close to an allowed electronic transition of the molecule, an enhancement in the scattering cross section occurs due to a resonance effect in the polarizability tensor. This enhancement is approximately (Kildal, et al., 1971)

$$(C_{\text{raman}})_{\text{res}} \sim (C_{\text{raman}})_{\text{nonres}} \times \frac{\omega_0^2}{(\omega_1 - \omega_0)^2 + \left(\frac{\Delta\omega}{2}\right)^2} \quad (3.44)$$

where

- ω_1 = the pump frequency (incident frequency)
- ω_0 = the electronic transition frequency
- $\Delta\omega$ = the line width of the electronic transition

3.4 Rayleigh and Mie Scattering

In scattering, the characteristics of the individual scattering elements and the statistical properties of the turbid medium greatly influence the intensity and geometric nature of the scattering. The geometrical structure of the medium is mainly characterized by two dimensionless parameters a/λ and l/λ where a is the average diameter of the particle, l is the distance between particles, and λ is the wavelength of the incident radiation. The laws of scattering differ considerably for cases when $a \ll \lambda$ and when the particle size is comparable to or larger than the wavelength ($a \geq \lambda$).

When $l \gg \lambda$, the particles can be considered as independent radiators. The particle positions are assumed to be random, thus, there will be no amplitude interference between the fields of individual particles, but only summation of scattered radiation intensities.

The most general scattering theory is that of Mie in which the particles are considered to radiate as higher order multipoles (quadrupoles, etc.). However, in the approximation when they can be treated as radiating dipoles, the theory of Rayleigh holds quite well.

The classical electromagnetic theory of scattering was first developed by Lord Rayleigh and applies to the case where:

1. The dimensions of the scattering particles are much smaller than the wavelength ($a \ll \lambda$).
2. The refractive index of the particles differs only slightly from that of the medium.
3. The particles scatter radiation independently of one another, this is only possible for $l \gg \lambda$.

Rayleigh scattering from the molecular atmosphere is important for it provides a method by which atmospheric densities may be derived from radar or lidar measurements. In addition it also provides a convenient, predictable background to which other scattering and absorption effects may be related. For wavelengths well separated from the absorption lines of the atmospheric constituents, the Rayleigh scattering cross section C_{ray} of an individual scattering center is given by (Collis, 1968)*

$$C_{\text{ray}} = \frac{8\pi}{3} \left(\frac{2\pi}{\lambda} \right)^4 \alpha^2 \frac{6 + 3\delta}{6 - 7\delta} \quad (3.45)$$

where

δ = depolarization factor due to the anisotropy of the atmosphere

α = molecular polarizability of scatterer

For the atmospheric gases, the factor δ has a value near 0.035, therefore the fraction

$$\frac{6 + 3\delta}{6 - 7\delta} = 1.061 \quad (3.46)$$

*Note the angular dependence has been integrated out.

The polarizability is approximately $2 \times 10^{-30} \text{ m}^3$ and thus

$$C_{\text{ray}} = 3.96 \times 10^{-44} \lambda^{-4} \text{ cm}^2 \quad (3.47)$$

where λ is expressed in centimeters for the microwave region ($\lambda = 1 \text{ cm}$)

$$C_{\text{ray}} = 3.96 \times 10^{-44} \text{ cm}^2 \quad (3.48)$$

while at the ruby wavelength ($\lambda = 0.694 \mu$)

$$C_{\text{ray}} = 1.71 \times 10^{-27} \text{ cm}^2 \quad (3.49)$$

The total scattering coefficient of a pure gaseous atmosphere K_s^{ray} is C_{ray} , the scattering cross section per molecule multiplied by N , the number density of molecular scatterers.

Thus

$$K_s^{\text{ray}} = N C_{\text{ray}} \quad (3.50)$$

This quantity K_s^{ray} is also called the Rayleigh attenuation coefficient. When K_s^{ray} is multiplied by the incident power density and the effective illuminated volume, the total power scattered in all directions from the incident radiation is obtained. For pure Rayleigh scattering, it can be shown that $3/8 \pi$ per steradian of this total will be scattered back toward the source. Thus, the volume backscattering coefficient for Rayleigh scatter is

$$B_{180}^{\text{ray}} = \frac{3}{8\pi} K_s^{\text{ray}} \quad (3.51)$$

Consider the following illustrative example. Let a transmitter be radiating power P_T from an antenna of gain G (power gain over isotropic). This will produce a power density (watts per square meter) at a distance R_1 (meters) of

$$\frac{P_T G}{4\pi R_1^2} \quad (3.52)$$

Most bodies, particles, and molecules subtend a small enough angle at the transmitter to be considered point targets. If the point target scatters isotropically with an effective cross section C_s (square meters), the scattered power density (flux) at a range R_2 from the particle is

$$\frac{P_T G}{4\pi R_1^2} \cdot \frac{C_s}{4\pi R_2^2} \propto \bar{S} \quad (3.53)$$

The power P_r (watts) returned to the receiver, intercepted by an antenna of effective area A (square meters) is (ignoring attenuation)

$$P_r = \frac{P_T G C_s A}{16\pi^2 R_1^2 R_2^2} \propto \bar{S} A \quad (3.54)$$

For the case of an electromagnetic wave with electric field intensity E_o incident upon a small dielectric sphere of refractive index n , the time averaged radiant flux of Rayleigh scattering can be written as (Kondratyev, 1969)

$$\bar{S} = \frac{\pi c (1 + \cos^2 \theta)}{16R^2 N\lambda^4} (n^2 - 1)^2 E_o^2 \quad (3.55)$$

where

$$\frac{E_o^2}{2\eta} \propto \frac{P_T G}{4\pi R^2} \frac{\text{watts}}{\text{m}^2} = \frac{\text{power radiated}}{\text{m}^2}$$

\bar{S} = the scattered energy per unit time per unit area perpendicular to the direction of scattered radiation at a distance R from the scattering particle at an angle θ with the incident radiation unpolarized

c = the speed of light

η = the (wave) impedance = $\sqrt{\frac{\mu}{\epsilon}}$
of the medium

The Mie theory is a comprehensive treatment of the scattering of a plane electromagnetic wave by a dielectric sphere. The expressions are quite complicated involving associated Legendre polynomials, Riccati-Bessel functions, and spherical Bessel functions. However, many useful approximations exist (Appendix C). Mie theory must be used whenever the particulate matter has dimensions of magnitude similar to the wavelength of the incident radiation. For large particles the elementary scattering cross section C_{mi} is of the order of twice the geometrical cross section. The scattering pattern in the Mie case does not resemble the symmetrical dipole pattern of Rayleigh scatter, but can be quite irregular and complicated due to the higher order multipole terms. In addition to the index of refraction, the results depend critically on the shape and size of the particle. Even a sphere has a complex angular dependence. In the case of a water droplet with a radius of 10^{-3} mm, the scatter is strongest in the forward direction, decreasing by a factor of 4 at $\theta = \pi/2$ and increasing slightly in the direction of $\theta = \pi$. Thus, for this case, forward scatter and direct backscatter are the most favorable observing angles. Mie scattering from a single particle does preserve the initial frequency and phase of the incident radiation. However, in an ensemble of particles which are (normally) randomly distributed, there is a loss of coherence.

The polarization of the scattered radiation is a complex function of the size parameter $\alpha_1 = 2\pi a/\lambda$ where a is the particle radius and λ the incident wavelength, but the degree of polarization is generally smaller than in Rayleigh scatter.

The ratio of the backscattered intensity to the total scattered intensity is a highly variable function of the particle size to wavelength ratio and the dielectric characteristics of the particle. Generally, Mie scattering is predominantly forward so that in an assemblage of particles of different sizes, K' is often less than one in the relation

$$B_{180}^{\text{Mie}} = K' K_s^{\text{Mie}} \quad (3.56)$$

where an approximation to K_s^{Mie} is presented in Appendix C.

Since the effects of particle size differences tend to average out in reasonable volumes, useful approximate values can be determined for K' and used in evaluating the return signal. Calculations performed at Stanford Research Institute (Collis, 1968) for water droplet distributions typical of natural water clouds give an average value of $K = 0.625$. Thus, from scattering theory one can detect the presence of cloud and haze layers, measure their height, shape, and in the absence of excessive attenuation, their thickness. Figure 4 shows the difference between B_{180}^{ray} and B_{180}^{Mie} for a clear standard atmosphere. The magnitude of Mie scattering generally depends on the aerosol concentration and, thus, varies with changing atmospheric conditions in contrast to molecular Rayleigh scattering which remains fairly constant.

The intensity of the backscatter for both types is given by

$$P_r = \frac{P_T c \tau B_{180}^A}{8\pi R^2} \exp \left\{ -2 \int_0^R \sigma(r) dr \right\} \quad (3.57)$$

where

P_r is the received power

P_T is the transmitted power

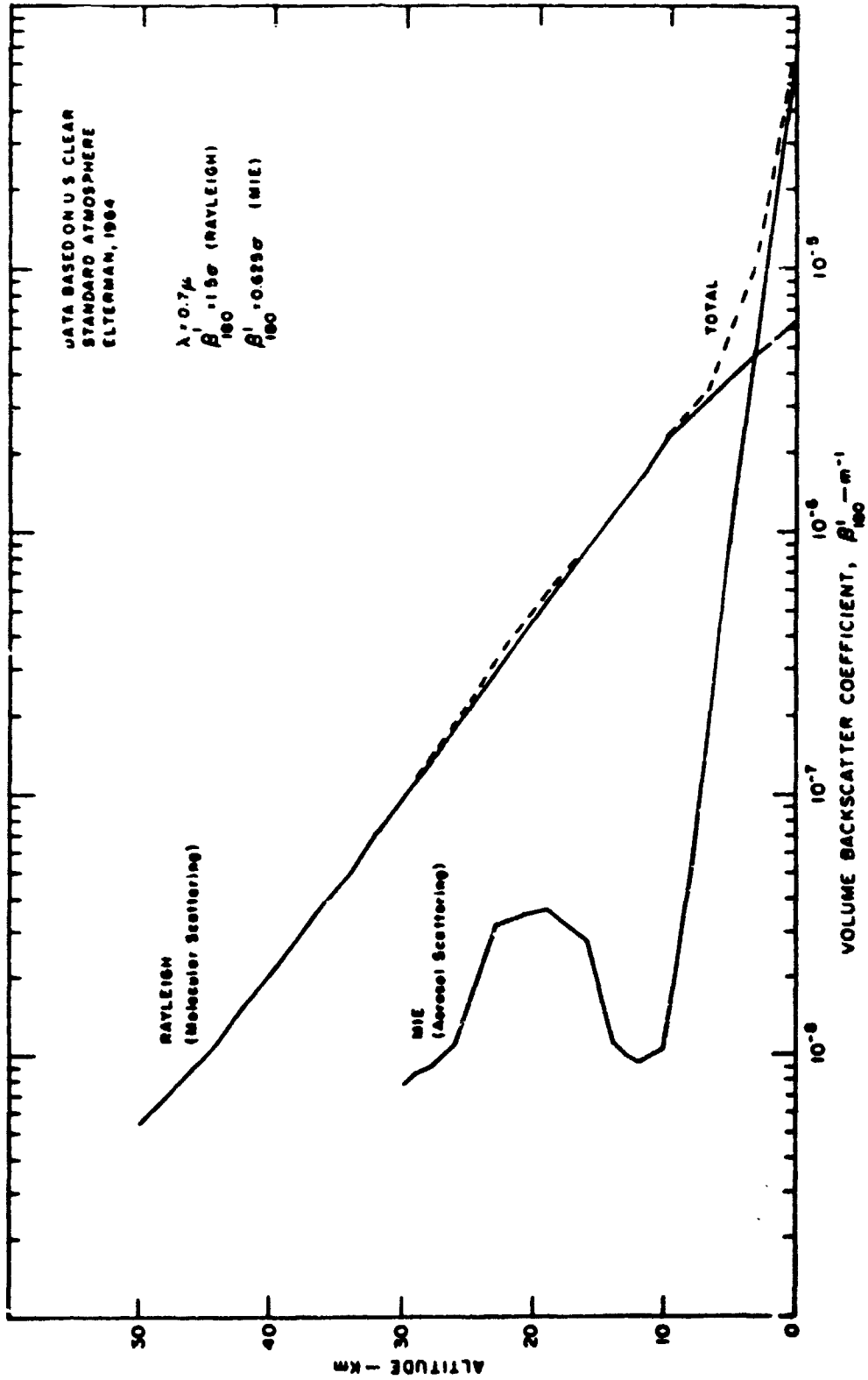


Figure 4: Volume backscatter coefficients for a clear standard atmosphere (Collis, R. T. H., 1968)

c is the speed of light

τ is the pulse duration

R is the range

B_{180} is the volume backscattering coefficient at range R

A is the effective receiver aperture

$\sigma(r)$ is the attenuation coefficient

3.5 Refractive Index

The bulk physical properties of the medium and of the scattering particles are characterized in general by a complex refractive index

$$m = n - i\chi \quad (3.58)$$

where n is the real refractive index and χ is directly proportional to the absorption coefficient.

The physical meaning of this complex refractive index is as follows: A plane wave of angular frequency

$$\omega = 2\pi f = \frac{2\pi c}{\lambda} \quad (3.59)$$

propagating along the z axis, must have the form

$$U = U_0 \exp [i(\omega t - Kz)] \quad (3.60)$$

in order to satisfy Maxwell's equations for time harmonic fields, where U is any of the field variables. The wave number K is then written as $K = K_0 m$ where $K_0 = \frac{\omega}{c} = \frac{2\pi}{\lambda}$ is the free space wave number.

One may write

$$\begin{aligned} U &= U_0 \exp[i\{\omega t - K_0(n - i\chi)z\}] \\ &= U_0 \exp[-K_0\chi z] \exp[i(\omega t - K_0nz)] \end{aligned} \quad (3.61)$$

From this it can be seen that if χ is not zero, there is a net attenuation of the wave. Then since radiation intensity I is proportional to the square of the field strength

$$I = I_0 \exp(-K_a Z) \quad (3.62)$$

where $K_a = 2K_0\chi = \frac{4\pi\chi}{\lambda}$, the coefficient of absorption.

This complex refractive index means that the atmosphere is a lossy medium (absorption taking place) and can be described in terms of a complex dielectric constant

$$\epsilon = \epsilon_1 - i\epsilon_2 \quad (3.63)$$

which will give rise to absorption which can be either non-resonant or resonant. In the case of non-resonant absorption, the real part of the dielectric constant decreases monotonically as the frequency is increased from zero to infinity. The classical theory of non-resonant absorption is that of Debye.

Debye (1929) considered the effect of an impressed electric field upon the dielectric constant of both non-polar and polar molecules; a polar molecule being one with a strong permanent dipole moment. He derived the result that polarizability is composed of two effects: The first due to the distortion of all the molecules by the impressed field and the second arising from an orientation effect exerted upon polar molecules (Bean, 1962).

Thus, the polarization $P(\omega)$ of a polar fluid under the influence of a high frequency radio wave is given by (Bean, 1962)

$$P(\omega) = \frac{\epsilon - 1}{\epsilon + 2} \frac{M_o}{\rho} = \frac{4\pi N_o}{3} \left[\alpha_o + \frac{\mu^2}{3kT} \frac{1}{1 + i\omega \tau_o} \right] \quad (3.64)$$

where

ϵ is the complex dielectric constant

M_o is the molecular weight

ρ is the density of the fluid

N_o is avogadro's number

α_o is the average polarizability of the molecules in the liquid assuming no interaction between molecules

μ is the permanent dipole moment

T is the absolute temperature

k is the Boltzmann's constant

τ_o is the relaxation time required for external field induced orientations of the molecules to return to random distribution after the field is removed

ω is $2\pi\nu$ where ν is the frequency of the external field

From Debye's analysis one can conclude that for external fields with frequencies less than 100 GHz, that $\omega\tau_o \ll 1$ and thus

$$P(\omega) \approx \frac{4\pi N_o}{3} \left[\alpha_o + \frac{\mu^2}{3kT} \right] \quad (3.65)$$

For non-polar gases $\mu = 0$ and

$$P(\omega) = \frac{4\pi N_o}{3} \alpha_o \quad (3.66)$$

For gases the dielectric constant is found to be very close to one so that $\epsilon + 2 = 3$. Thus

$$P(\omega) = \frac{\epsilon - 1}{\epsilon + 2} \frac{M_o}{\rho} = \frac{4\pi N_o}{3} \alpha_o \quad (3.67)$$

and

$$\epsilon - 1 = 4\pi N_o \alpha_o \frac{\rho}{M_o} \quad (3.68)$$

From the perfect gas law

$$P_i = \frac{R_o}{M_o} \rho \cdot T \quad (3.69)$$

one may write

$$\epsilon - 1 = 4\pi N_o \alpha_o \frac{P_i}{R_o T} = K_1 \frac{P}{T} \quad (3.70)$$

Likewise for polar gases

$$\epsilon - 1 = K_2 \frac{P}{T} \left(A + \frac{B}{T} \right) \quad (3.71)$$

where K_1 , K_2 , A , B are constants.

For a mixture of gases Dalton's law of partial pressures is assumed to hold with the result that one can sum the effects of polar and non-polar gases and thus

$$\epsilon - 1 = \sum_{i=1}^j K_{1i} \frac{P_i}{T} + \sum_{g=1}^l K_{2g} \frac{P_g}{T} \left(A_g + \frac{B_g}{T} \right) \quad (3.72)$$

For the troposphere, one need only consider the effects of dry air (non-polar gases) and water vapor (a polar gas) such that

$$\epsilon - 1 = K_1 \frac{P_d}{T} + K_2 \frac{P_w}{T} \left(A + \frac{B}{T} \right) \quad (3.73)$$

where

P_d is the pressure of dry air

P_w is the pressure of water vapor.

Since the real refractive index is defined as

$$n = \sqrt{\epsilon_1} \quad (3.74)$$

and since the above Equation (3.74) is real. Then

$$\epsilon_1 - 1 = K_1 \frac{P_d}{T} + K_2 \frac{P_w}{T} \left(A + \frac{B}{T} \right) \quad (3.75)$$

Then one can write

$$n = \sqrt{\epsilon_1} = \sqrt{1 + (\epsilon_1 - 1)} = \frac{\epsilon_1 - 1}{2} + 1 \quad (3.76)$$

or

$$n - 1 \approx \frac{\epsilon_1 - 1}{2} \quad (3.77)$$

which is true for $\epsilon_1 - 1 \ll 1$ or $(n^2 - 1 \ll 1)$. Thus

$$n - 1 = \frac{K_1}{2} \frac{P_d}{T} + \frac{K_2}{2} \frac{P_w}{T} \left(A + \frac{B}{T} \right) \quad (3.78)$$

Since in the atmosphere n is very close to one, it is common to define a more sensitive parameter, N .

N , the refractivity, is defined as

$$N \equiv (n - 1) \times 10^6 \quad (3.79)$$

and one then has the general expression for refractivity of the atmosphere (Bean, 1962)

$$N = 77.6 \frac{P_d}{T} + 72 \frac{P_w}{T} + 3.75 \times 10^5 \frac{P_w}{T^2} \quad (3.80)$$

This is an accurate expression since the influence of other gases, mainly carbon dioxide, cause less than a 0.02 percent error. Assuming normal atmospheric parameters, the above equation is considered valid for frequencies up to 30 GHz. The equation relates the bulk atmospheric parameters to the microscopic properties of the atmosphere which for large numbers of particles make up the macroscopic dielectric properties of the atmosphere.

It can also be written in the form (Lusignan, et al., 1969)

$$N = 223 \rho_a + 334 \rho_w + 1.74 \times 10^6 \rho_w / T \quad (3.81)$$

where the density of dry air ρ_a and water vapor density ρ_w are expressed in Kg/m^3 and the temperature T in degrees Kelvin.

3.6 Reflection

This process is a wave interaction with the fluctuations of refractive index. For a discontinuity in the refractive index of air, the coherent scatter which arises can be approximated with a reflection coefficient. This process generally occurs when $l \ll \lambda$. This form of attenuation arises mainly from aerosols since in general, they have a higher index of refraction than air, making a sharper discontinuity. This reflection mechanism may be found in a region of temperature inversion where an enhanced aerosol concentration may exist. The layer of air containing the aerosols will then serve as a coherent scattering (reflecting) mechanism of incident electromagnetic energy due to the discontinuity (Hajovsky, et al., 1966). This process is dependent on the bulk atmospheric parameters of density, temperature, and humidity which determine the refractive index, and is much less frequency dependent than the processes of absorption and emission.

The theoretical signal level of a radar echo received due to reflection from a layer of infinite extent is given by Hajovsky and Lagrone (1966) as

$$P_R = \frac{P_T G^2 \lambda^2 \Gamma^2}{64\pi^2 R^2} \quad (3.82)$$

where

P_R = signal level of radar echo

P_T = power radiated

G = gain of the antenna above an isotropic radiator

λ = wavelength of radiated energy

Γ^2 = power reflection coefficient of layer

R = range

The power reflection coefficient Γ^2 is given by (Hajovsky, et al., 1966)

$$\Gamma^2 = \left[\frac{\Delta N}{\Delta z} \frac{\lambda}{8\pi} \right]^2 \times 10^{-12} \quad (3.83)$$

for a plane layer with refractive index gradient, $\Delta N/\Delta z$, and vertical incidence.

The expression for a linear refractive index gradient is

$$\frac{\Delta N}{\Delta z} = 1.5 \left(\frac{n_1^2 - 1}{n_1^2 + 2} \right) \frac{C}{\rho} \quad (3.84)$$

where

C = (mass) density of the aerosols air mixture in micrograms per cubic centimeter ($\mu\text{g}/\text{cm}^3$)

ρ = density of the suspended particle material in grams per cubic centimeter (g/cm^3)

n_1 = refractive index of the aerosols (Hajovsky and Lagrone, 1966)

This formulation for $\frac{\Delta N}{\Delta z}$ holds only for aerosols of diameter much less than the wavelength of incident radiation, where the refractive index of air is unity, and no interaction between suspended particles occur.

The reflection coefficient may also be expressed from Fresnel's formulas. For normal incidence the fraction of incident flux which is reflected in a given direction from the interface between two media is defined as (Jenkins and White, 1957)

$$K_r = \left| \frac{m - 1}{m + 1} \right|^2 = \frac{(n - 1)^2 + \chi^2}{(n + 1)^2 + \chi^2} \quad (3.85)$$

where m is the complex refractive index ($m = n - i\chi$).

CHAPTER IV

MICROWAVE ABSORPTION

4.1 General

The absorption of microwave energy from a radio wave by atmospheric gases is due to the transition from one molecular rotation energy level to another caused by the electromagnetic wave. For this process to occur with radiation of a particular wavelength, the molecule or atom must have an appreciable absorption cross section at that wavelength, and the process must have a high probability compared to the other processes that are also energetically possible.

There are two critical parameters involved in each energy level transition. The first is the frequency associated with the transition energy. This may be determined from a knowledge of the energy levels or from direct measurement. However, the energy differences are very small for absorption lines in the microwave spectrum. The error involved in taking the difference of two nearly equal values is large. Thus, for this reason direct measurement of resonant frequency is preferable when possible (Straiton, et al., 1960).

The second critical number is the line width constant associated with the frequency spread of the absorption line. This value should be determined by direct measurement for the most reliable results (Straiton, et al., 1960). Uncertainty as to the value of $\Delta\nu$ (the line width constant) has been a major stumbling block in the theoretical calculation of absorption.

Some of the atmospheric gases giving rise to (microwave and infrared) emission and absorption are: O_2 , H_2O , O_3 , CO , SO_2 , N_2O , CH_4 , and NO_2 (see Figure 5), however, the effects of almost all of

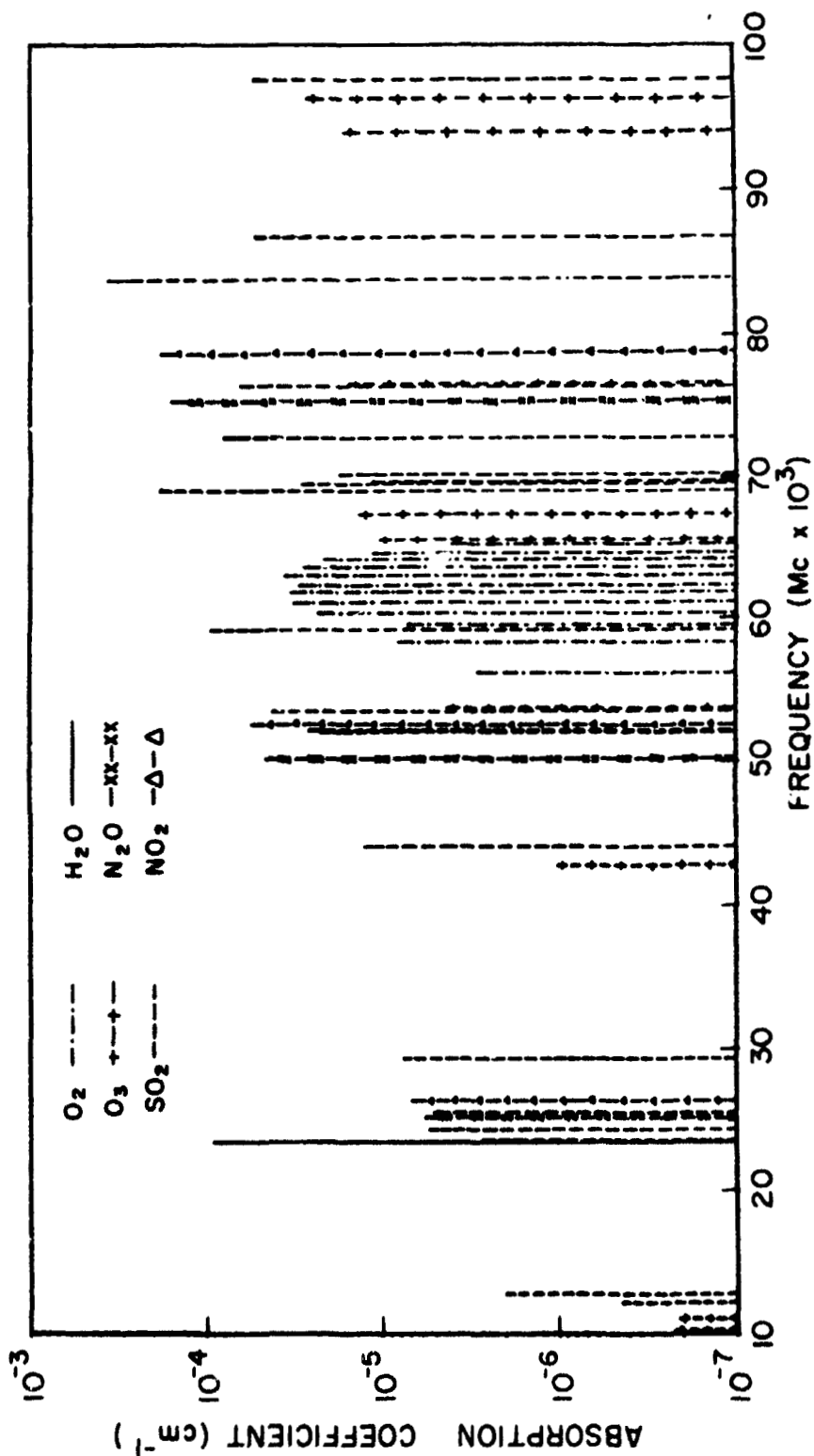


Figure 5: Rotational frequencies and absorption coefficients of atmospheric gases between 10 GHz and 100 GHz (Ghosh, S. N. and Edwards, H. D., 1956)

these gases are normally negligible due to their low concentration. Molecular absorption in the centimeter and millimeter wavelength bands is primarily due to absorption by oxygen and water vapor (see Figures 6 and 7). Water vapor and oxygen molecules have permanent electric and magnetic dipole moments respectively, which when excited by an electromagnetic wave, oscillate and rotate with many degrees of freedom, each associated with a quantized energy level $h\nu$. Thus, the molecules absorb discrete amounts of energy from the wave and are raised to higher energy levels. In returning to a lower level, they reradiate energy isotropically, and therefore, the net result is an attenuation of the incident wave. This process is called resonant absorption.

Water vapor has resonances at frequencies of about 22 GHz ($\lambda \approx 1.35$ mm.) and 183 GHz ($\lambda \approx 1.64$ mm) (see Figures 6 and 7). Oxygen has 25 closely spaced resonances occurring in the region of 60 GHz ($\lambda \approx 0.5$ cm). However, because of pressure broadening, the wings of the individual lines overlap to form a continuous region of absorption at elevations near sea level (Altshuler, et al., 1968).

Oxygen absorption dominates over that of water vapor except in the immediate wavelength region of the water vapor line, even though the absorption coefficients of the two gases are of the same order of magnitude. This occurs as a consequence of the large density ratio of oxygen to water vapor in the atmosphere.

The shapes and intensities of the water vapor resonances are dependent upon atmospheric temperature, pressure, and the partial pressure of water vapor, whereas the shapes of the oxygen resonance lines are a function only of atmospheric temperature and pressure since

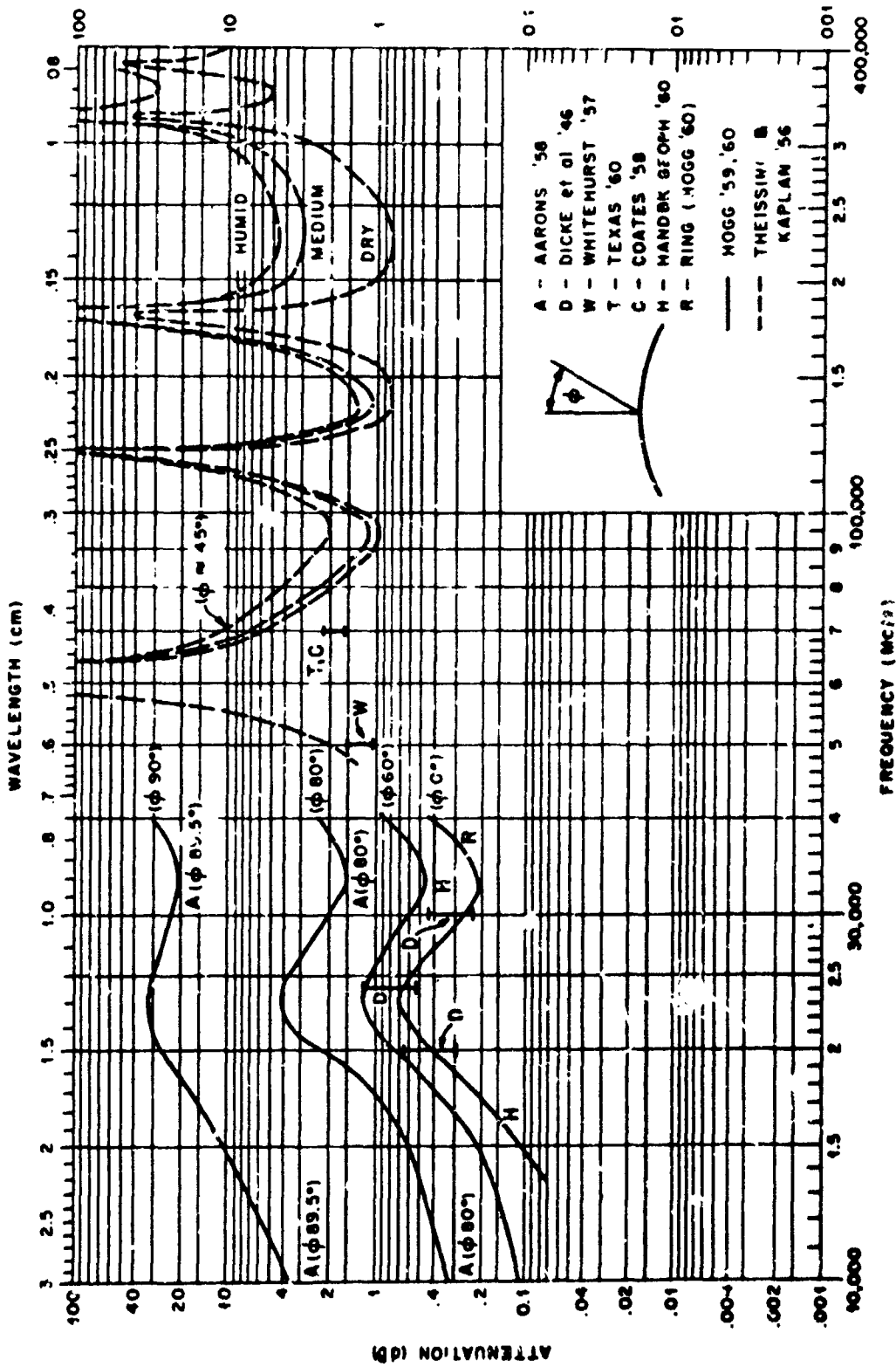


Figure 6: Total attenuation one way transmission through the atmosphere (Meyer, J. W., 1966); reprinted by permission of the Institute of Electrical and Electronic Engineers Inc.)

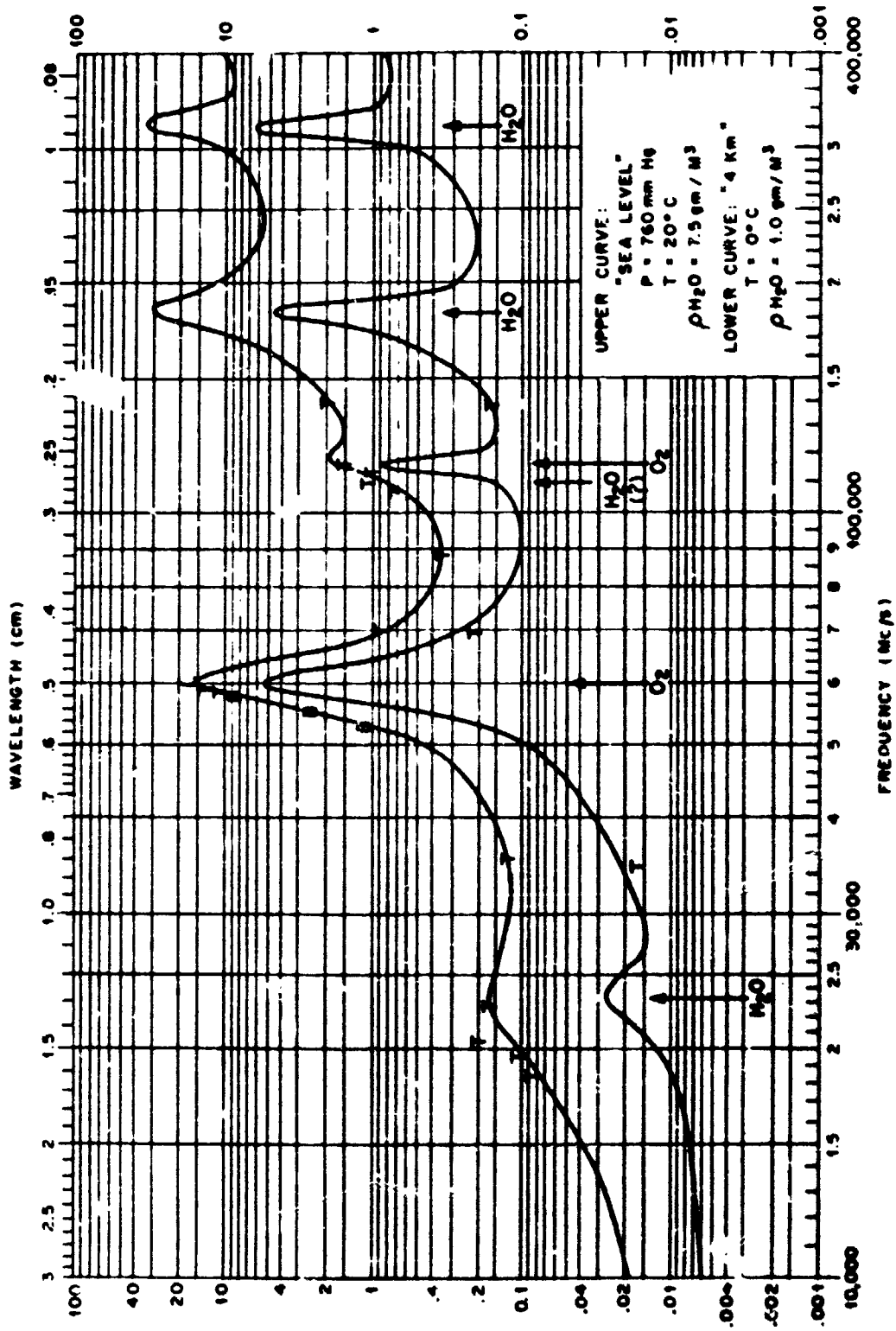


Figure 7: Attenuation per kilometer for horizontal propagation (Meyer, J. W., 1966; reprinted by permission of the Institute of Electrical and Electronic Engineers, Inc.)

the concentration of oxygen is known (Altshulter, et al., 1968). Absorption (at 15 - 35 GHz) on clear summer days is caused principally by water vapor, while in winter days depending on the latitude, the water vapor content is so low that oxygen absorption becomes predominant (Altshulter, et al., 1968). Half of the absorption by water vapor and oxygen from the surface up to the stratosphere takes place in the first 3.2 km which comprises 32 percent of the atmospheric mass. This is due to the pressure broadening of the complex of oxygen lines near 5 mm. Less than one percent of the absorption is due to the atmosphere above 17 km (Shimabukuro, 1966).

In the portions of the microwave spectrum far removed from a water vapor absorption line, the attenuation is primarily controlled by the wings of the submillimeter (far infrared) lines of O_2 and H_2O . The effect on an absorption line can be seen in Figure 8. In the frequency range 50 to 130 GHz, the first 12 lines (line numbers in the order of increasing frequency) make a small contribution to the total absorption and the line numbers 21 through 76 make approximately the same contribution as the first 20 lines. This set of curves is based on the assumption that the line width constant is 0.1 cm^{-1} (3 GHz) for all the lines (see Figure 9). It is now believed that the line width will vary from line to line, thus the curves most likely will increase more rapidly with frequency than is shown. This is so since Benedict and Kaplan (1964) point out that there is considerable theoretical and experimental evidence that the line width for the various water vapor lines is different depending on the rotational states involved. With the imposing array of lines which influence millimeter absorption, the general effect would be that of having a greater increase in absorption with frequency as the shorter millimeter wavelengths are approached.

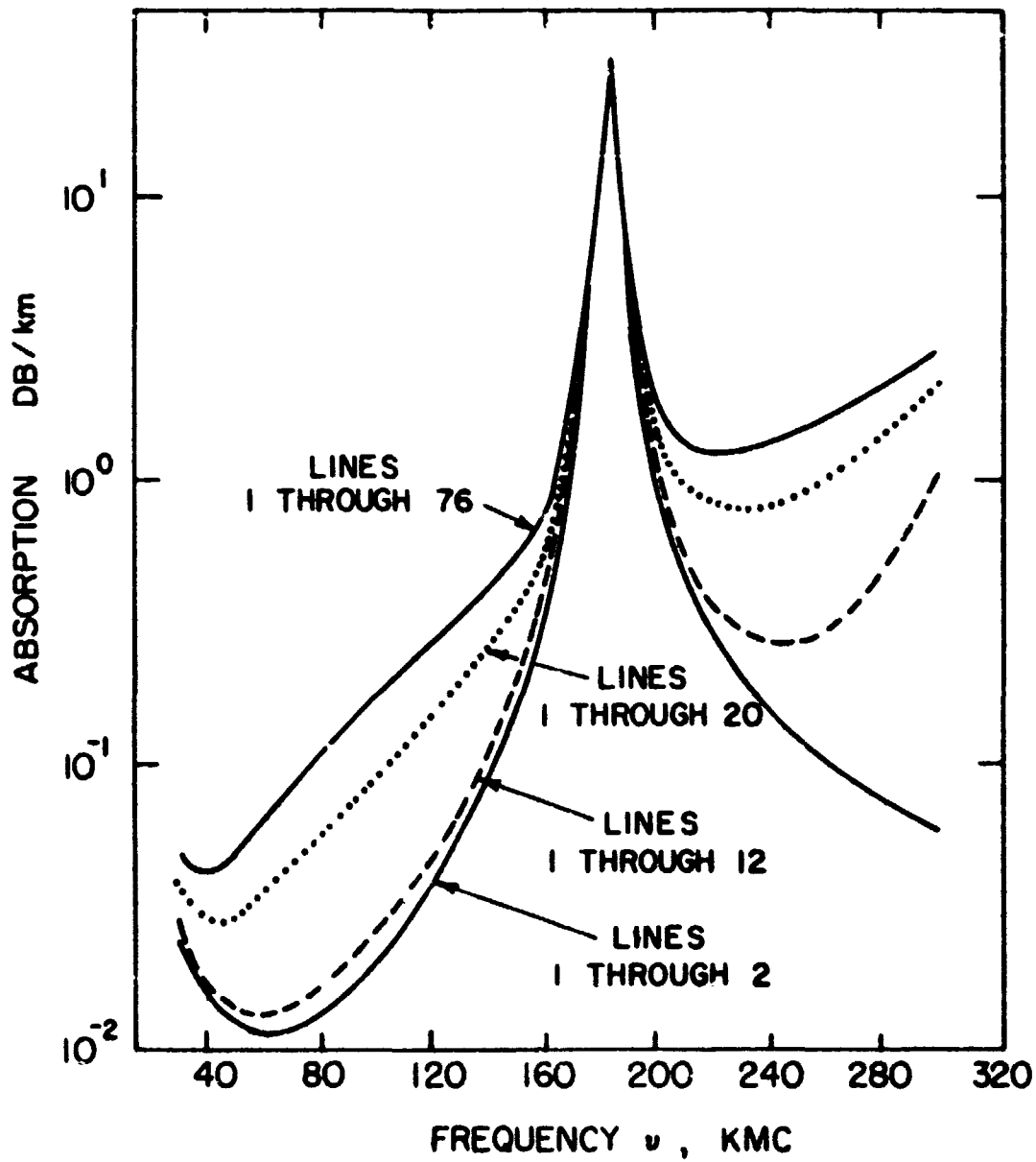


Figure 8: Calculated water vapor absorption for 7.5 g/m^3 with $\Delta\nu/c = 0.1$ (Straiton, A. W. et al, 1960; reprinted by permission of the Institute of Electrical and Electronic Engineers, Inc.)

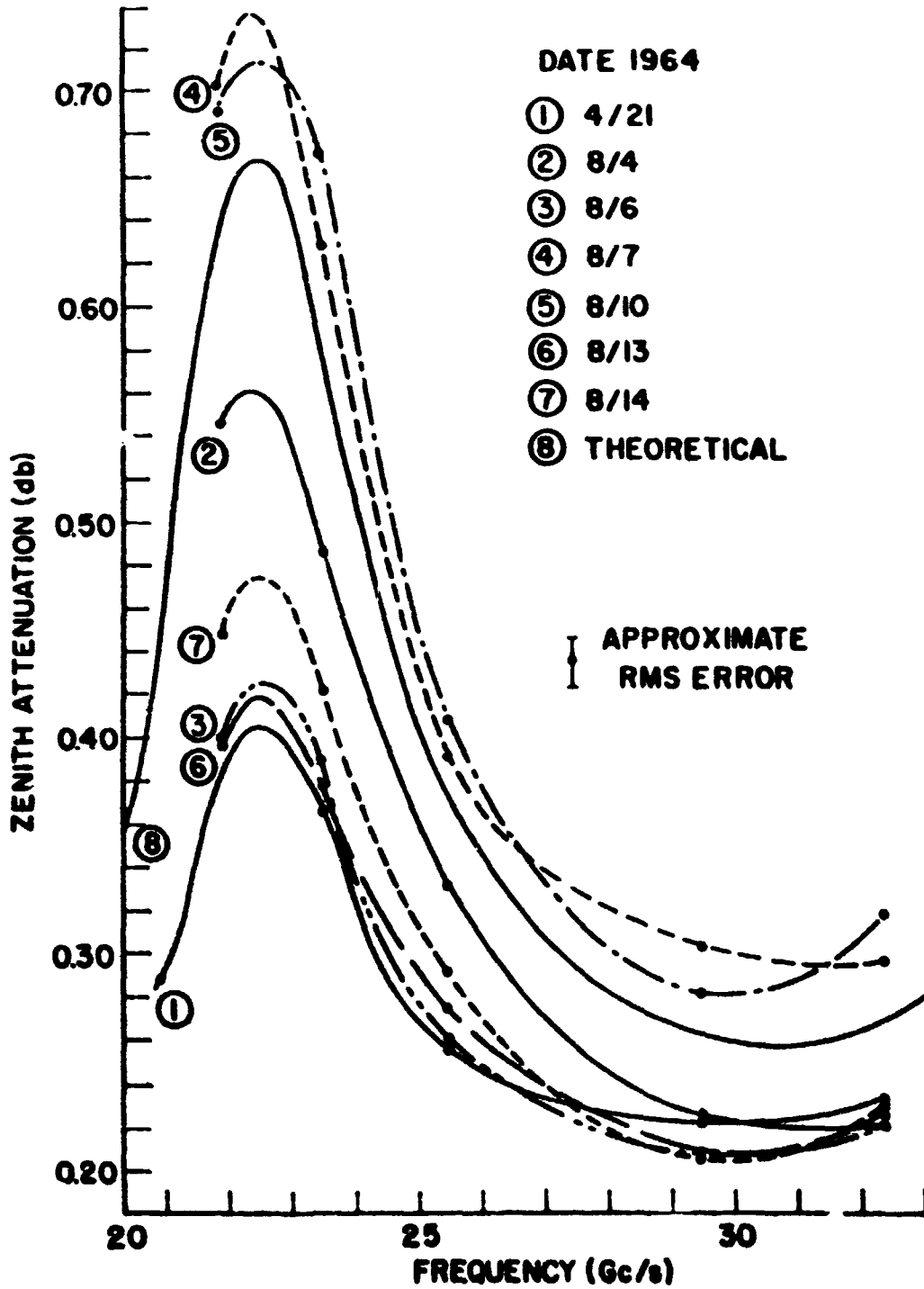


Figure 9: Measured atmospheric absorption spectra (Welch, 1968)

Molecular absorption has been analyzed by many theorists. The form presented by Van Vleck (1947) using the Van Vleck-Weisskopf (1945) equation has accounted most closely for observed absorption data. Quantitative prediction of the lines has been less successful. Most attempts to adapt the Van Vleck-Weisskopf equation to observed absorption measurements use a single line broadening constant throughout the absorption spectrum of oxygen and another for water vapor in spite of experimental and theoretical evidence to the contrary because of the scarcity of information about the exact parameters to use. The Van Vleck-Weisskopf equation considers the broadening effect of collisions between molecules. Pressure or collision broadening is the dominant process determining the width of spectral lines in the range of pressures that occur from the surface of the earth to the upper stratosphere. Under these conditions, the absorption calculated at any frequency that does not coincide with a strong absorption maximum is influenced appreciably by the wings of many lines and can vary widely depending on the broadening assumed for each of them.

The major assumption made by Van Vleck and Weisskopf was in the collision process where they assumed that after the instantaneous impact, the oscillator variables are distributed according to a Boltzmann distribution. The Van Vleck formulas give the absorption per unit distance given the pressure, temperature, and water vapor content of a sample of the atmosphere. However, uncertainties still exist in the absorption line widths which are temperature and pressure dependent, and thus, limit the accuracy of the computed absorption. At pressures found in the lower atmosphere, the Lorentz (pressure) line widths are of the same order of magnitude as their separation.

The general quantum mechanical formula for the absorption coefficient K_a for microwaves of frequency ν is (Van Vleck, 1947)

$$K_a = 10^6 (\log_{10} e) \frac{8\pi^3 \nu N}{3hc} \frac{\sum_i \sum_j \left\{ |\mu_{ij}|^2 f(\nu_{ij}, \nu) e^{-\frac{E_j}{kT}} \right\}}{\sum_j e^{-\frac{E_j}{kT}}} \quad (4.1)$$

where μ_{ij} is the matrix element of the dipole moment connecting two discrete states i, j which have energy E_i, E_j respectively.

ν_{ij} is the frequency of the corresponding spectral line

N is the number of molecules per cubic centimeter

ν is the frequency of the incident radiation

The factor $10^6 (\log_{10} e)$ converts K_a into units of decibels per kilometer, and the factor $f(\nu_{ij}, \nu)$ is the form factor which determines the shape of the absorption line and is given by

$$f(\nu_{ij}, \nu) = \frac{\nu}{\pi \nu_{ij}} \left[\frac{\Delta\nu}{(\nu_{ij} - \nu)^2 + \Delta\nu^2} + \frac{\Delta\nu}{(\nu_{ij} + \nu)^2 + \Delta\nu^2} \right] \quad (4.2)$$

$\Delta\nu$ is the line width and is proportional to the number of collisions per unit time. In order to calculate $\Delta\nu$ theoretically, the collision cross section must be known.

From the fact that

$$h\nu_{ij} = E_i - E_j = -h\nu_{ji} \quad (4.3)$$

we have

$$f(\nu_{ij}, \nu) = -f(\nu_{ji}, \nu) \quad (4.4)$$

The absorption due to a single line in the millimeter or submillimeter regions may then be written as

$$K_a^{ij}(\nu, \nu_{ij}) = (10^6 \log_{10} e) \frac{8\pi^3}{3hc} \frac{N\nu}{G} \cdot [\exp(-E_i/kT) - \exp(-E_j/kT)] |\mu_{ij}|^2 f(\nu, \nu_{ij}) \quad (4.5)$$

where

K_a^{ij} = absorption at frequency ν due to an absorption line centered at ν_{ij} in dB/km

$G = \sum_j e^{-E_j/kT}$, the rotational partition function

h, k, c = Planck's constant, Boltzmann's constant, speed of light

Then the factor

$$\exp(-E_i/kT) - \exp(-E_j/kT) \quad (4.6)$$

may be expanded as

$$\begin{aligned} & \exp(-E_i/kT) [1 - \exp(-[E_j - E_i]/kT)] \\ & = \exp(-E_i/kT) [1 - \exp(h(-\nu_{ji})/kT)] \end{aligned} \quad (4.7)$$

Then for microwave frequencies

$$h\nu_{ij} \ll kT \quad (4.8)$$

or $1 - \exp(-h\nu_{ji}/kT) = \frac{h\nu_{ji}}{kT}$

Thus

$$K_a^{ij}(\nu, \nu_{ij}) = (10^6 \log_{10} e) \frac{8\pi^3}{3hc} \frac{N\nu}{G} \cdot \frac{h\nu_{ji}}{kT} \cdot \exp(-E_i/kT) |\mu_{ij}|^2 f(\nu, \nu_{ij}) \quad (4.9)$$

The factor $\nu\nu_{ij} f(\nu, \nu_{ij})$ may be defined as

$$F(\nu, \nu_{ij}) \equiv \nu\nu_{ij} f(\nu, \nu_{ij}) \quad (4.10)$$

Then the modified Van Vleck-Weisskopf line shape is given by

$$F(\nu, \nu_{ij}) = \nu^2 \Delta\nu \left[\frac{1}{(\nu - \nu_{ij})^2 + \Delta\nu^2} + \frac{1}{(\nu + \nu_{ij})^2 + \Delta\nu^2} \right] \quad (4.11)$$

where

$$F(\nu, \nu_{ij}) \approx \begin{cases} \nu_{ij}^2 / \Delta\nu & \nu = \nu_{ij} \\ 2 \Delta\nu & \nu \gg \nu_{ij} \\ (2 \Delta\nu / \nu_{ij}^2) \nu^2 & \nu_{ij} \gg \nu \end{cases} \quad (4.12)$$

Gross (1955) derived a kinetic theory line shape factor assuming that after impact, the oscillators have a Maxwellian distribution of velocities, but that their positions are unchanged. This line shape formula takes the same form as the Van Vleck-Weisskopf formula at resonance, but seems to provide better agreement with measurements in the high frequency wing.

The Gross modified line shape is

$$F(\nu, \nu_{ij}) = \nu^3 \nu_{ij} \frac{4\Delta\nu}{(\nu_{ij}^2 - \nu^2)^2 + 4\nu^2 \Delta\nu^2} \quad (4.13)$$

where

$$F(\nu, \nu_{ij}) = \begin{cases} \nu_{ij}^2 / \Delta\nu & \nu = \nu_{ij} \\ \nu^3 \nu_{ij} 4\Delta\nu / [\nu^4 + 4\nu^2(\Delta\nu)^2] & \nu \gg \nu_{ij} \\ \nu^3 & \nu_{ij} \gg \nu \\ 4\Delta\nu / \nu_{ij}^3 & \nu_{ij} \gg \nu \end{cases} \quad (4.14)$$

A third line shape proposed by Schulze-Tolbert (1963) is

$$F(\nu, \nu_{ij}) = \nu^2 \frac{(\Delta\nu)^{0.65}}{|\nu_{ij} - \nu|^{1.65} + (\Delta\nu)^{1.65}} \quad (4.15)$$

where

$$F(\nu, \nu_{ij}) = \begin{cases} \nu_{ij}^2 / \Delta\nu & \nu = \nu_{ij} \\ (\nu^2 / \nu^{1.65}) (\Delta\nu)^{0.65} & \\ = \nu^{0.35} (\Delta\nu)^{0.65} & \nu \gg \nu_{ij} \\ (\nu^2 / \nu_{ij}^{1.65}) (\Delta\nu)^{0.65} & \nu_{ij} \gg \nu \end{cases} \quad (4.16)$$

4.2 Water Vapor Absorption

Barrett and Chung (1962) refined the expression of Van Vleck on the basis of the experimental findings of Becker and Autler (1946) and the theoretical calculations of Benedict and Kaplan (1959). Barrett and Chung give the pressure and temperature dependence of the water vapor line widths as

$$\Delta\nu = \Delta\nu_0 \left(\frac{P}{1013.25} \right) \left(\frac{318}{T} \right)^x (1 + .0046\rho) \quad (4.17)$$

where x was calculated by Benedict and Kaplan (1964) for H₂O - H₂O collisions to be 0.614. Calculations by Benedict and Kaplan (1959) for

for the case of H₂O - N₂ broadening resulted in X_{N₂} = 0.626 for the temperature range of 220 to 300°K. These calculations indicate a value of Δν_o = 0.09019 cm⁻¹ (2.704 GHz) at T = 300°K. Benedict and Kaplan (1964) also found that X_{O₂} is approximately equal to X_{N₂}. These considerations indicate then, that the temperature and pressure dependence of the water vapor line widths in air may be represented as (Westwater, 1965)

$$\Delta\nu_{\text{H}_2\text{O}} \sim \frac{P_{\text{H}_2\text{O}}}{P} \left(\frac{T}{T_0}\right)^{-X_{\text{H}_2\text{O}}} + \frac{B_{\text{O}_2} P_{\text{O}_2}}{P} \left(\frac{T}{T_0}\right)^{-X_{\text{O}_2}} + \frac{B_{\text{N}_2} P_{\text{N}_2}}{P} \left(\frac{T}{T_0}\right)^{-X_{\text{N}_2}} \quad (4.18)$$

where P_m is the partial pressure of the mth molecular species and B_m represents the relative effectiveness of the mth constituent over H₂O - H₂O collisions in producing water vapor broadening. The reference temperature is given by T_o and P = P_{H₂O} + P_{O₂} + P_{N₂} is approximately the total pressure of the air.

The expression used by Chung and Barrett for K_a, the absorption coefficient at a frequency ν_o = 22.235 GHz is

$$K_a = \frac{3\pi^2 N}{3ckTG} |\mu_{1.35}|^2 \nu^2 \exp\left(-\frac{E_{5,-1}}{kT}\right) \left[\frac{\Delta\nu}{(\nu - \nu_0)^2 + \Delta\nu^2} + \frac{\Delta\nu}{(\nu + \nu_0)^2 + \Delta\nu^2} \right] + \frac{16\pi^2 N \nu^2 \Delta\nu}{3hc G} \sum_{i=0}^{\infty} \sum_{j=0}^{\infty} \frac{|\mu_{ij}|^2}{\nu_{ij}} \exp\left(-\frac{E_j}{kT}\right) \quad (4.19)$$

where

$$G = \sum_{j=0}^{\infty} \sum_{\tau=-j}^j [2 - (-1)^{|\tau|}] (2j + 1) \exp\left(-\frac{E_j}{kT}\right)$$

$E_{5,-1}$ is the energy involved in the transition (J : 5 - 1 → 6 - 5) and has the energy equivalent value of 446.39 cm^{-1} (Dennison, 1940) and

$|\mu_{1.35}|^2$ is the square of the dipole moment determinant for the above transition and has a value of 5.6×10^{-37} esu (King, et al., 1947).

The first term is a single resonant term representing the water vapor line at 1.35 cm (22.235 GHz), the second term represents the absorption in the wings of all lines below 1.35 cm. In the second term, the fact that $\nu \ll \nu_{ij}$ for all lines other than the 1.35 cm line has been used to write

$$f(\nu_{ij}, \nu) \sim 2\nu(\Delta\nu)/\pi \nu_{ij}^3 \quad (4.20)$$

Then using Van Vlecks (1947) expression for G

$$G = 0.034 T^{3/2} \quad (4.21)$$

they arrived at

$$K_a(1.35 \text{ cm}) = 1.05 \times 10^{-28} \frac{N\nu^2}{T^{5/2}} \exp\left(\frac{-644}{T}\right) \left[\frac{\Delta\nu}{(\nu - \nu_0)^2 + \Delta\nu^2} + \frac{\Delta\nu}{(\nu + \nu_0)^2 + \Delta\nu^2} \right] + 1.52 \times 10^{-52} \frac{N\nu^2 \Delta\nu}{T^{3/2}} \text{ cm}^{-1} \quad (4.22)$$

It should be pointed out that the equation that appears in Barrett and Chung's paper has two misprints; the above expression has been corrected.

The line width constant was obtained from Becker and Autler's (1946) data by Barrett and Chung as

$$\Delta\nu = 2.62 \times 10^9 \frac{(P/760)(1 + .0046\rho)}{(T/318)^{.625}} H_z \quad (4.23)$$

where

P is the total pressure in mm Hg

ρ is the density of H₂O in g/m³

and T is normalized to 318°K since Becker and Autler's measurements were made at this temperature.

One problem inherent in this formulation is that the nonresonant term was derived under the assumption that the half-width $\Delta\nu$ was the same for all lines. However, it is now recognized that the absorption at frequencies far removed from the resonance line exceeds the theoretical predictions. Thus, Barrett and Chung increased the nonresonant term by a factor of 5 to match Becker and Autler's measurements.

Croom (1965) used the Barrett and Chung coefficient for an indepth study of water vapor absorption at 22.235 GHz and in a similar fashion obtained an absorption coefficient for the 1.64 mm line. This equation is:

$$K_a(1.64 \text{ mm}) = 6.46 \times 10^{-29} \frac{N\nu^2 e^{-\frac{200}{T}}}{T^{5/2}} \cdot \left[\frac{\Delta\nu}{(\nu - \nu_0)^2 + \Delta\nu^2} + \frac{\Delta\nu}{(\nu + \nu_0)^2 + \Delta\nu^2} \right] + 1.8 \times 10^{-52} \frac{N\nu^2 \Delta\nu}{T^{3/2}} \text{ cm}^{-1} \quad (4.24)$$

where $\Delta\nu$ is the same as Equation (4.23).

For the above expression, the first term is due to the resonant effect and the second term represents an approximation to the effects

of the wings of the 13.5 mm line and the numerous sub-millimeter H₂O lines in the vicinity of 1.64 mm.

4.3 Oxygen Absorption

The absorption of microwaves is also caused by 25 oxygen lines at about 60 GHz (5 mm) and a single line at 118.75 GHz (2.53 mm). Under sea level conditions, pressure broadening of the lines near 5 mm results in their merging together to form one line, however, observations from about 30 km should enable them to be resolved. The oxygen absorption coefficient obtained from Van Vleck's formula is

$$K_a = \frac{(10^6 \log_{10} e) \frac{4\pi^3 \nu N}{3ckT}}{\sum_n 3(2n+1) e^{-\frac{E_n}{kT}}} \sum_{n \text{ odd}} [\gamma_n] \quad (4.25)$$

$$[\gamma_n] = \left\{ 2 \left| \langle \nu_{n^+} \rangle \cdot \langle i(\nu_{n^+}; \nu) | \mu_{n^+}^2 + 2 \left| \langle \nu_{n^-} \rangle \langle f(\nu_{n^-}; \nu) | \mu_{n^-}^2 + F(\nu) \mu_{no}^2 \right. \right\} e^{-\frac{E_n}{kT}} \quad (4.26)$$

where

$$f(\nu_{ij}, \nu) = \frac{\nu}{\pi \nu_{ij}} \left[\frac{\Delta \nu}{(\nu_{ij} - \nu)^2 + \Delta \nu^2} + \frac{\Delta \nu}{(\nu_{ij} + \nu)^2 + \Delta \nu^2} \right] \quad (4.27)$$

$$F(\nu) = \lim_{\nu_{ij} \rightarrow 0} [\nu_{ij} f(\nu_{ij}, \nu)] = \frac{2\nu \Delta \nu}{\pi(\nu^2 + \Delta \nu^2)} \quad (4.28)$$

$$\mu_{n^+}^2 = \frac{4\beta^2 n(2n+3)}{n+1} \quad (4.29)$$

$$\mu_{n^-}^2 = \frac{4\beta^2 (n+1)(2n-1)}{n} \quad (4.30)$$

$$\mu_{no}^2 = \frac{8\beta^2 (n^2 + n + 1)(2n+1)}{n(n+1)} \quad (4.31)$$

and $\beta = \frac{he}{4\pi mc}$

The selection rules for the fine structure transitions permit transitions of the form $(J = n) \rightarrow (J = n + 1)$ and $(J = n) \rightarrow (J = n - 1)$. The corresponding frequencies for these transitions are ν_{n^+} and ν_{n^-} .

Meeks and Lilley (1963) modified the expression to the following:

$$K_a(\nu, P, T) = C_1 \frac{P\nu^2}{T^3} \sum_{n \text{ odd}} S_n \exp\left(\frac{-E_n}{kT}\right) \quad (4.32)$$

where

$$S_n = F_{n^+} |\mu_{n^+}|^2 + F_{n^-} |\mu_{n^-}|^2 + F_0 |\mu_{n0}|^2$$

$$F_{n^\pm} = \frac{L}{(\nu_{n^\pm} - \nu)^2 + \Delta\nu^2} + \frac{\Delta\nu}{(\nu_{n^\pm} + \nu)^2 + \Delta\nu^2}$$

$$F_0 = \frac{\Delta\nu}{\nu^2 + \Delta\nu^2}$$

$$\mu_{n^+}^2 = \frac{n(2n+3)}{n+1}$$

$$\mu_{n^-}^2 = \frac{(n+1)(2n-1)}{n}$$

$$\mu_{n0}^2 = \frac{2(n^2 + n + 1)(2n + 1)}{n(n + 1)}$$

The exponent in the Boltzmann factor is

$$\frac{E_n}{kT} = 2.06844 \frac{n(n+1)}{T} \quad (4.33)$$

and $C_1 = 2.6742$ for K_a in decibels/km.

Meeks and Lilley (1963) formed an empirical expression for $\Delta\nu$

$$\Delta\nu(P, T) = \alpha_2 P [0.21 + 0.78 \beta_2] \left(\frac{300}{T}\right)^{0.85} \quad (4.34)$$

where $\alpha_2 = 1.95 \text{ (MHz/sec)(mm of Hg)}^{-1}$, $\beta_2 = 0.75$, and P is in units of mm of Hg.

This empirical expression for the collision line width parameter can also be written as

$$\Delta\nu = g(h) \left(\frac{P}{P_0}\right) \left(\frac{T}{T_0}\right)^{-K'} \text{ GHz} \quad (4.35)$$

where P_0 is the standard pressure at the surface of the earth (760 mm Hg), T_0 is a reference temperature (300°K) and K' indicates the temperature dependence. The altitude factor $g(h)$ is

$$g(h) = \begin{cases} g_1 & 0 \leq h \leq h_1 \\ g_1 + (g_2 - g_1) \frac{(h - h_1)}{h_2 - h_1} & h_1 \leq h \leq h_2 \\ g_2 & h_2 < h \end{cases} \quad (4.36)$$

as can be seen, Meeks and Lilley (1963) used values of $g_1 = 0.60 \text{ GHz}$, $g_2 = 1.17 \text{ GHz}$, $h_1 = 8 \text{ km}$, $h_2 = 25 \text{ km}$, and $K' = 0.85$.

At altitudes above 50 km, Doppler broadening of the absorption lines becomes comparable to collisional broadening and must be considered. The expression from Townes and Schawlow (1955) for the Doppler line width is

$$\Delta\nu_D = 1.15 \times 10^{-6} \nu (T/T_0)^{0.5} \text{ GHz} \quad (4.37)$$

The shape of the Doppler broadened line is different from the collision broadened line. However for simplicity, it can be assumed that both shapes are defined by the equation for the collision broadened line and the resulting line width at least up to 60 km is $\Delta\nu + \Delta\nu_D$ (Meeks and Lilley, 1963).

For oxygen absorption, the nonresonant absorption coefficient, 0.0064 dB/km, must be added to the resonant term to obtain the total attenuation coefficient. This term accounts for almost all of the oxygen absorption at 10 GHz.

CHAPTER V
INFRARED ABSORPTION

5.1 General

The principal constituents of the atmosphere are nearly transparent in the visible and infrared, but the minor atmosphere constituents CO_2 , H_2O , and O_3 have strong absorption bands in the infrared, and therefore, according to Kirchoff's law, also emit infrared radiation from those bands.

In the infrared region CO_2 bands exist at 1.4 μ , 1.6 μ , 2.0 μ , 2.7 μ , 4.3 μ , 4.8 μ , 5.2 μ , and 15.0 μ . There are seven principal regions of water vapor absorption in the near infrared beyond 0.9 μ . These are due to rotation-vibration bands near 0.94, 1.1, 1.38, 1.87, 2.7, 3.2, and 6.3 μ . Although each of these regions is sometimes referred to as a band, more than one rotation vibration band may be present in each region. For example, the 2.7 μ band of water vapor actually consists of the close lying fundamentals ν_1 and ν_3 (Howard, et al., 1956). Other bands are due to methane at 7.65 μm and N_2O at 7.78 μm .

The absorption (or emission) in the far infrared (50-1000 μm) occurs because of rotational transitions of the molecules while the higher energy absorption bands in the infrared region of 1 to 20 μm occur because the molecules are vibrating, as well as rotating.

In a gaseous medium a typical infrared absorption band is composed of numerous closely spaced narrow absorption lines due to the combined vibrational and rotational energy levels of the absorbing molecules. This leads to the absorption coefficient changing rapidly

with wavelength, and thus, the averaged transmittance over a wavelength interval containing several individual lines may not vary exponentially with the quantity of absorber. However, it is possible to obtain a transmission function which relates the average transmittance over a small wavelength interval to an averaged absorption coefficient and the quantity of absorber. These transmission functions have been derived by Elsasser (1938) for an array of lines whose intensity and spacing varies slowly with wavelength and by Goody (1952) for an array of lines with statistically random spacing and a uniform or exponential intensity distribution. Carbon dioxide absorption has a line structure which can be represented by the Elsasser model while water vapor and ozone are best represented by the Goody model.

5.2 The Elsasser Model of an Absorption Band

Elsasser (1938) considered the case of an idealized absorption band consisting of an infinite array of equally intense, equidistant lines, each with a Lorentz shape given by (Howard, et al., 1956)

$$K_a = \frac{S_o}{\pi} \frac{\Delta\nu}{(\nu - \nu_o)^2 + \Delta\nu^2} \quad (5.1)$$

where the half width, $\Delta\nu$, and average intensity, S_o , are considered constant for each line. Because the pattern is periodic in frequency (for equidistant lines) the fractional absorption in any period is the same as the fractional absorption for the entire band. If the line centers of the individual lines are located at $\nu = 0, \pm d, \pm 2d, \dots$ and each line has the Lorentz shape, then the absorption coefficient will be given by (Howard, et al., 1956)

$$K_a = \sum_{n=-\infty}^{\infty} \frac{S_o}{\pi} \frac{\Delta\nu}{(\nu - nd)^2 + \Delta\nu^2} \quad (5.2)$$

which can be expressed as

$$K_a = K(x) = \frac{S_o}{d} \frac{\sinh \beta}{\cosh \beta - \cos x} \quad (5.3)$$

using the Mittag-Leffler theorem where $x = \frac{2\pi\nu}{d}$ and $\beta = \frac{2\pi\Delta\nu}{d}$. If one assumes that the incident intensity is constant throughout the spectrum, the fractional absorption for the entire band becomes (Howard, et al., 1956)

$$A = \frac{1}{2\pi} \int_{-\pi}^{\pi} (1 - \exp[-K(x)W]) dx \quad (5.4)$$

where W is the absorber concentration in atmos cm.* The absorption, A_ν , at any frequency in the vicinity of an absorption line can be expressed as

$$A_\nu = 1 - \frac{I_\nu}{I_o} = 1 - e^{-K_a W} \quad (5.5)$$

where I_ν is the intensity of the radiation of frequency ν transmitted by a sample having absorber concentration W , I_o is the intensity of the incident radiation of frequency ν and is assumed to be constant for all frequencies in the vicinity of the absorption line and K_a is the absorption coefficient at frequency ν .

When the lines are far apart compared to their half width ($d \gg \Delta\nu$ or β is small) one can write

$$K_a = K(x) = \frac{S_o \beta}{2d \sin^2(x/2)} \quad (5.6)$$

* An atmos cm is the path length in cm which would contain the same number of molecules if the gas were at STP.

and integrate to obtain (Appendix D)

$$A = \operatorname{erf} \frac{(\pi S_0 \Delta \nu W)^{1/2}}{d} \quad (5.7)$$

where

$$\operatorname{erf}(y) = \frac{2}{\sqrt{\pi}} \int_0^y \exp(-t^2) dt$$

The fractional absorption of the band can best be represented by

$$A = \operatorname{erf} \left(\frac{lW}{2} \right)^{1/2} \quad (5.8)$$

where

$$l = \frac{2\pi \Delta \nu S_0}{d^2} \quad (5.9)$$

and is a generalized absorption coefficient for the band.

The restrictions of the idealized band are relaxed and the fractional absorption A is considered to be the absorption at the center of an interval ν_1 to ν_2 containing several lines that are of approximately equal intensity. If one assumes that there is no contribution to the absorption at the center of this interval from lines outside the interval, the expression can be written (Howard, et al., 1956)

$$A(\nu_1, \nu_2) = \operatorname{erf} \left(\frac{l(\nu_1, \nu_2)W}{2} \right)^{1/2} \quad (5.10)$$

where $l(\nu_1, \nu_2)$ is the generalized absorption coefficient defined above and depends on the average line spacing $d(\nu_1, \nu_2)$ and the average line strength $S_0(\nu_1, \nu_2)$ in the interval. The applicable quantity $l(\nu_1, \nu_2)$ can be determined empirically over the band and is considered to be a function of ν , varying slowly over the band, the rapid

variation of the primary absorption coefficient K_a from line to line having been obliterated (Howard et al., 1956).

4.3 The Goody Model of an Absorption Band

In 1950, Cowling (1950) took data on the line positions and relative intensities for the pure-rotational absorption lines of water vapor from Randall, Dennison, Ginsberg, and Weber (1937). He then assumed the Lorentz line shape for the individual lines and computed the absorption as a function of absorber concentration for six wavelength regions (Howard et al., 1956).

These absorption curves were so similar however that Cowling was led to the conclusion that in atmospheric work complication is avoided and small error is involved if a single absorption curve is used at all wavelengths (Howard et al., 1956).

This led Goody (1952) to conclude from inspection of the diagrams of Randall et al. that the only common feature of these ranges is a nearly random distribution of line intensities and positions (Howard et al., 1956).

Goody then postulated the so-called statistical or random model for a disordered band and showed that this model fits quite well the earlier computations of Cowling. He considered the fractional transmission at the center of an interval of frequencies $n\delta$ wide, where n is the number of lines in the interval; and δ is the mean line spacing. The interval is considered sufficiently wide so that there is no absorption at its center due to lines outside of the interval. It is postulated that all arrangements of line positions are equally probable, that is, the line spacings are random and it is further postulated that there is no correlation between line positions and line strengths. The line strengths are assumed to be given by the following function (Howard et al., 1956)

$$P(S_o) = \frac{1}{\sigma} \exp\left(\frac{-S_o}{\sigma}\right) \quad (5.11)$$

where $P(S_o)dS_o$ is the probability that a given line has a strength in the range S_o to $S_o + dS_o$ and σ is the mean line strength in the interval. The individual lines of the band are assumed to have the Lorentz shape (Howard et al., 1956).

With these assumptions about the nature of the disordered band, one can show that the transmission (at the center of the interval considered, when the radiation traverses the concentration, W , of absorbing gas along the transmission path (W))(Howard et al., 1956) is given by

$$T(\Delta\nu, W\sigma) = \exp\left[\frac{-W\sigma\Delta\nu}{\delta(\Delta\nu^2 + \frac{W\sigma\Delta\nu}{\pi})^{1/2}} \right] \quad (5.12)$$

Thus the fractional transmission in such an interval of an absorption band depends on the mean line spacing, the mean line strength, and the half width as well as on the optical thickness of the absorber. This random model can be applied to the near infrared absorption bands of H_2O . The half width $\Delta\nu$ is assumed to be the same for all of the H_2O individual absorption lines although it depends on pressure and temperature, also the average line spacing is assumed to be the same for all of the H_2O bands. Then for a fixed value of W , the transmission at a given frequency is considered to depend on the mean line strength σ in the neighborhood of this frequency. The mean line strength is thought to be a slowly varying function of frequency over the band and can be specified in terms of W_o (the value of W necessary to yield a transmission of 1/2 at a given frequency). Thus in the Goody model as in the Elsasser model, the rapid variation over each individual line of the primary

absorption coefficient K_a has been obliterated. The combination of the two functions $T(\Delta\nu, W\sigma)$ and $\sigma(\nu)$ then describes the transmission process for this particular band (Howard et al., 1956). It has been shown by Plass (1958, 1960) that under conditions when absorption at the line centers is virtually complete, W and pressure P enter into transmission functions only as a product. The transmission function is termed then the strong line approximation. When the absorption is small at all wavelengths, including the line centers, the transmittance is independent of pressure and depends only on the absorber concentration. This is the weak line approximation.

Beyond a band head where there are no line centers, there may nevertheless be absorption from the wings of strong lines near the middle of the band. Also in spectral regions where lines from more than one absorber are present, the combined transmittance is taken as the product of the transmittances calculated for the separate absorbers, provided that there is no correlation between the separate arrays of lines.

The weak line approximation is given as (Bradford et al., 1964)

$$T = e^{-\beta Y} = \exp \frac{-S_o W}{d} \quad (5.13)$$

$$\text{where } \beta = \frac{2\pi\Delta\nu}{d} \quad \text{and } Y = \frac{S_o W}{2\pi\Delta\nu}$$

The strong line approximation is given as (Bradford et al., 1964)

1) For the Elsasser model
$$T = 1 - \operatorname{erf} \left(\frac{\beta^2 X}{2} \right)^{1/2} \quad (5.14)$$

2) For the Goody model
$$T = \exp \left[\left(\frac{2}{\pi} \beta^2 Y \right)^{1/2} \right] \quad (5.15)$$

The wing function for the Lorentz line shape is

$$T = \exp \left[-WP \sum_i \frac{S_i}{(\nu_i - \nu)^2} \frac{\alpha_0}{\pi} \right] \quad (5.16)$$

CHAPTER VI

METHODS OF DETECTION

6.1 General

The techniques of microwave spectroscopy and radio astronomy offer a potentially valuable method for studying water vapor in the upper atmosphere. It is useful to characterize these techniques which might be adopted for water vapor detection as active and passive. The passive method involves only a receiver which can monitor the thermal emission (spectra) of the water vapor molecules, or measure the attenuation of an external source (usually the sun) by atmospheric water vapor. The active method is similar to radar, in which a transmitter-receiver system is used to excite a region and then monitor the return. In this method, the incident radiation may be characterized by amplitude (or power), frequency (or wavelength), phase, direction, polarization, and coherence. Any of these characteristics may be changed in the process of absorption, scatter, or reradiation. Thus the receiver can be designed to detect one or more changes of the incident radiation and from these changes, inferences are drawn about the content of the region.

There are three basic types of observation in the passive sense: measurement of the spectrum of absorption of the sun's radiation by an atmospheric constituent, remote (with respect to the earth's surface) measurement of the emission spectrum of a constituent, and measurement monochromatically of the zenith angle (or slant range) dependence of the absorption or emission of the atmosphere.

The emission spectrum measurement utilizes the assumption that the atmosphere may be considered to approximate a medium in

local thermodynamic equilibrium (LTE) at least up to about 70 km. Above this, departures from LTE occur because the collisional deactivation lifetime of an excited molecule becomes comparable with its radiative lifetime.

Thermal emission, when observed from any region of the atmosphere is a function of the distribution of temperature and concentration of the emitting gas along the atmospheric path under observation. Thus an estimate of concentration can be made by observing the sky temperature or apparent emission intensity of an atmospheric constituent. In this type of measurement, one requires a reference temperature measurement.

In the active method, microwave oscillators or lasers are set at the molecular resonances of the constituent to be measured. Since an orders of magnitude increase in reemitted signal may be present, the return from the given atmospheric constituent may be isolated. Knowledge of the line shape permits probing in various parts of the line and thus differential absorption can provide returns that can also yield information on concentration profiles. In general, since the absorbed energy must be at a frequency fixed by the molecular characteristic, the source or transmitter should be tunable.

At the present, the main probing techniques just described can be used in various frequency ranges which include microwave, infrared, and visible ranges. There are certain strengths and weaknesses associated with each of these frequency ranges for the detection process.

Infrared and visible frequencies are still largely a fair weather tool as they cannot penetrate significant rain, fog, or cloud cover. For this reason, it would appear (on an operational basis) that microwave

frequencies are superior for overall detection and actual measurements from the ground (or at least within the troposphere).

Some of the factors which complicate the detection problem are: absorption and emission from atoms and molecules not of the species of interest, spatial and temporal inhomogeneities, scattering by air or land, clouds, rain, snow, dust, etc.

The absorption of radio waves in the lower atmosphere is the result of both free molecules and suspended particles such as dust grains and water droplets occurring in fog and rain. The effect of absorption by liquid water droplets becomes increasingly severe with increasing frequency. Clouds and precipitation attenuate electromagnetic waves through both absorption and scattering processes. Since cloud droplets are generally less than 100 μm in diameter, the Rayleigh approximation holds at microwave frequencies. Clouds are the most difficult systems to model since they contain water in all three states: gas (uncondensed water vapor), liquid (water droplets), and solid (ice crystals).

The relative humidity in water clouds is for all practical purposes 100 percent. The amount of uncondensed water vapor in clouds approximately doubles for each 10°C increase in temperature. Thus the water vapor content can vary from $\sim 4 \text{ g/m}^3$ at 0°C to $\sim 23 \text{ g/m}^3$ at 25°C .

The attenuation rate for uncondensed water vapor of 0.014 dB/km at a wavelength of 1.5 cm for each g/m^3 of water vapor content (Dicke, 1946) can lead to several tenths of a decibel per kilometer attenuation due to the water vapor alone. Thus attenuation from water clouds is much larger than that of ice clouds. Moreover the losses for both cases, are due principally to absorption rather than scattering. Thus, the attenuation depends more on total liquid water content than on droplet size distribution.

In the lower 30 km of the atmosphere, both molecular and aerosol scatter are observed. Thus scattering from aerosols must be taken into account when considering ground-based active measurements.

If the diameter of the particles is much less than the wavelength of radiated energy and the echoes from the individual scatterers are assumed to arrive at the antenna at the same time, but with random phase, then the radar echo signal level P_R from a volume of these individual scatterers is (Hajovsky and Lagrone, 1966)

$$P_R = \frac{P_T A_e \tau c \pi^4}{8\lambda^4 R^2} \left| \frac{\epsilon - 1}{\epsilon + 2} \right|^2 \sum_i N_i D_i^6 \quad (6.1)$$

where

A_e is the effective area of the antenna

τ is the pulse length

c is the speed of light

N_i is the number of particles per unit volume of i^{th} size group

D_i is the average diameter of the aerosols in the i^{th} size group

This formula holds only under the assumptions that: 1) the region containing the aerosols is large enough so that the volume illuminated by the radar beam is completely filled with the suspended particles; 2) the number of particles or aerosols per unit volume in the region is considered to be constant; and 3) the particles are considered to be perfect spheres.

The major equipment problem areas include sensitivity, absolute accuracy, spectral response, and directional response of the antenna. In addition, each application has constraints of cost, size, weight, power requirements, availability and operational simplicity.

Receiver sensitivity may be characterized by the receiver noise temperature T_R , the antenna temperature T_A , the bandwidth B , integration time τ , and a constant α which is usually in the range 1-3. Thus the equivalent rms fluctuations at the receiver input ΔT_{rms} is (Staelin, 1969)

$$\Delta T_{rms} = \frac{\alpha(T_A + T_R)}{\sqrt{B\tau}} \text{ } ^\circ\text{K} \quad (6.2)$$

This equation may be used to estimate an ultimate limit to receiver sensitivity. For example, a radiometer in space viewing the earth would see an antenna temperature T_A of $\sim 300^\circ\text{K}$. For a noiseless receiver ($T_R = 0$) with one second integration time, and $B = 10^8$ Hz, $\Delta T_{rms} = 0.03 - 0.09^\circ\text{K}$ depending on the value of α . If 1°K sensitivity is sufficient, then an integration time as short as 0.004 seconds may be used. These limits have a strong bearing on the ultimate spatial resolution and coverage which can be obtained by radiometers in space (Staelin, 1969).

Receiver noise temperatures are in the range of several hundred degrees at 3 cm wavelength to about 20,000 $^\circ\text{K}$ at 3mm wavelength. At wavelengths longer than 3 cm, receiver noise temperatures of less than 150°K can be obtained with solid state parametric amplifiers and this capability is being extended to wavelengths near 1cm (Staelin, 1969). Absolute accuracies of 1°K are readily obtainable and values of approximately $0.1 - 0.2^\circ\text{K}$ can be obtained with great care (Staelin, 1969).

For amplifiers other than low noise amplifiers, bandwidths ranging from 1 to 10^{10} Hz can be obtained over most of the microwave region of the spectrum while most parametric or other low noise amplifiers have instantaneous bandwidths of approximately 200 MHz or less (Staelin, 1969).

The directional response of antennas varies considerably depending upon wavelength and antenna size. The half-power beam-width of most antennas is approximately $1.3\lambda/D$ where λ is the wavelength and D is the antenna diameter. The sidelobe level should be small and in general, the antenna must be custom built. Some applications require scanned antennas (This can be done mechanically or electrically (phased array)). The advantages of mechanical scanning include a superior multi-frequency capability, lower antenna losses, and electronic simplicity. Electrical scanned antennas are more compact, need have no moving parts, and can scan more rapidly (Staelin, 1969).

6.2 Resonant Absorption

6.2.1 Passive Configuration

In this method, the integrated water vapor concentration is measured along a path through the atmosphere by monitoring the absorption of radiation from a natural source (generally the sun).

The equation describing this process for a horizontally stratified atmosphere and a flat earth is (Meeks and Lilley, 1963)

$$T_b = T_s \exp \left[- \int_h^{\infty} \sigma(x) \cos \phi dx \right] \quad (6.3)$$

where

T_b is the antenna temperature related directly to signal and noise power observed by an antenna with an infinitesimally narrow beam.

T_s is the brightness temperature of a source external to the measurement region (generally the sun).

h is the height of the antenna above the earth's surface.

ϕ is the angle between zenith and the direction of observation.

$\sigma(x)$ is the atmospheric attenuation coefficient at slant range x .

The sensitivity of the absorption measurement improves with the amount of water vapor in the path up to unit optical depth ($d\tau = K_a dz$) thus there exists a unique path length for maximum sensitivity. According to Croom (1964), this measurement is about 10 times more sensitive to small concentrations of water vapor than is the measurement of an emission line. This is due to the greater number of unexcited molecules to that number of excited molecules. This method is the most direct and least expensive solution to the detection problem and can be used to obtain water vapor profiles in principle by taking integrated water vapor measurements at several altitudes.

This method and others can be used to make observations from the ground, from space, and by line of sight (occultation) measurements. A discussion of these observations follow.

6.2.1.1 Ground Based Observations (resonant absorption-passive)

Microwave observations are made of crude total water vapor content using broad band radiometers and correlating the attenuation in certain $\Delta\lambda$ with ground based humidity measurements. The general procedure is to observe the signal level on a number of days and to plot the signal strength as a function of the measured water vapor content of the lower atmosphere. The slope of this line provides the water vapor losses and the ordinate or Y axis intercept provides the oxygen loss (Straiton et al., 1960). Using this data to predict attenuation under other conditions suffers not only from the difficulties of the spectral characteristics of the emitting source having to be assumed or determined separately, but also the composition and other properties of the

atmosphere as a function of altitude must likewise be assumed or measured. The separation of the absorption into water vapor and oxygen components then depends on these factors whose effects depend in turn on the details of the theory used.

Another experimental method is to measure the total attenuation of an external source of radiation by an atmospheric constituent. In the lower atmosphere this method has been used to study water vapor, oxygen, and ozone although water vapor and oxygen are now more commonly studied by emission techniques, which are discussed in the next section. However, in the upper atmosphere where the concentration of water vapor is small, the absorption measurements made from a space platform may be the only method feasible.

Advantages of both methods are the following: very sensitive to concentrations in the troposphere; simplicity; low power consumption; easy accessibility of data; no need to create radiation.

Disadvantages of the attenuation method are the following: frequency of receiver and antenna limited to those of the molecular transitions; requires accurate knowledge of absorption line strength; lack of sensitivity to concentrations in the upper atmosphere due to the bulk of earth's atmosphere attenuating signal; requires inversion of an integral equation to extract data. Disadvantages of the correlating method are that it is a very crude method although simple to employ and lack of sensitivity to concentrations in the upper atmosphere.

6.2.1.2 Observations From Above the Surface (Resonant Absorption-Passive)

This type of observation can monitor the absorption spectra of water vapor if the antenna is viewing an external source (sun, moon,

star, etc.). If the antenna is not fixed on a source, then the emission spectra of the atmosphere will be seen.

The upward viewing experiment is the most appealing configuration for measuring water vapor from a rocket or balloon. The radiometer will measure the radiation absorption due to the water vapor along the upward slant path. The intensity of absorption should decrease and approach zero as the rocket altitude increases since the concentration of water vapor is thought to decrease greatly above 90 km. This decrease in intensity when contrasted against the height of the rocket or vehicle should determine the relative water vapor concentration.

The main reason for using an absorption experiment from space is due to the enhanced sensitivity to concentrations above 30 km. The disadvantages are as follows: the equipment must have greater sensitivity and frequency stability to monitor the less broadened lines; restrictions on volume, weight, and power available; a data transmission system must be included; and an elevated instrumentation platform (rocket, balloon, satellite, etc.) is required. The main problem for a space based absorption experiment is to maintain the antenna fixed on the source throughout the flight. Another problem to be considered is that the integration time will have to be quite fast in order to use a rocket, yet the sensitivity of a radiometer when viewing the solar disc for example, is low unless the integration time is long. Thus, there exists a difficult compromise between sensitivity and integration speed.

4.2.1.3 Satellite Occultation (resonant absorption-passive)

In occultation, a satellite-borne radiometer receives the radiation emitted from another satellite (active resonant absorption), from the atmosphere (passive resonant emission), or from the sun (or other

natural source) along a ray path (passive resonant absorption). The ray path may be identified by the height (Tangent height) of the point (Tangent point) closest to the surface of the earth (see figure 10).

An important quantity measured in the occultation experiment is the radio refractivity. This occurs since radio waves propagate in the atmosphere not with the speed of light c , but with a reduced speed V_p given by

$$V_p = c/n \quad \text{where} \quad (6.4)$$

n is the refractive index

The modulus of refraction or refractivity N , is proportional to both the air density and to the water vapor density (see equation 3.81). The changes in refractive index have two effects on the radio waves. First, the phase velocity of the propagated wave front changes differentially causing the actual ray path to be deviated from the straight ray to a curved ray path (this is due to the atmospheric refractive index gradient). Second, the path appears to be longer since the waves travel slower, that is, the waves take a longer time to traverse the path and therefore, there are more wavelengths along the path. Thus, in its travel over the curved path, the wave suffers an overall phase retardation ϕ_s given by (Tank, 1969)

$$\phi_s = \frac{10^{-6}}{\lambda} \int N(s) ds \quad (6.5)$$

where

λ is the radiation wavelength

ds is an element of the curved path

$N(s)$ is the modulus of refraction

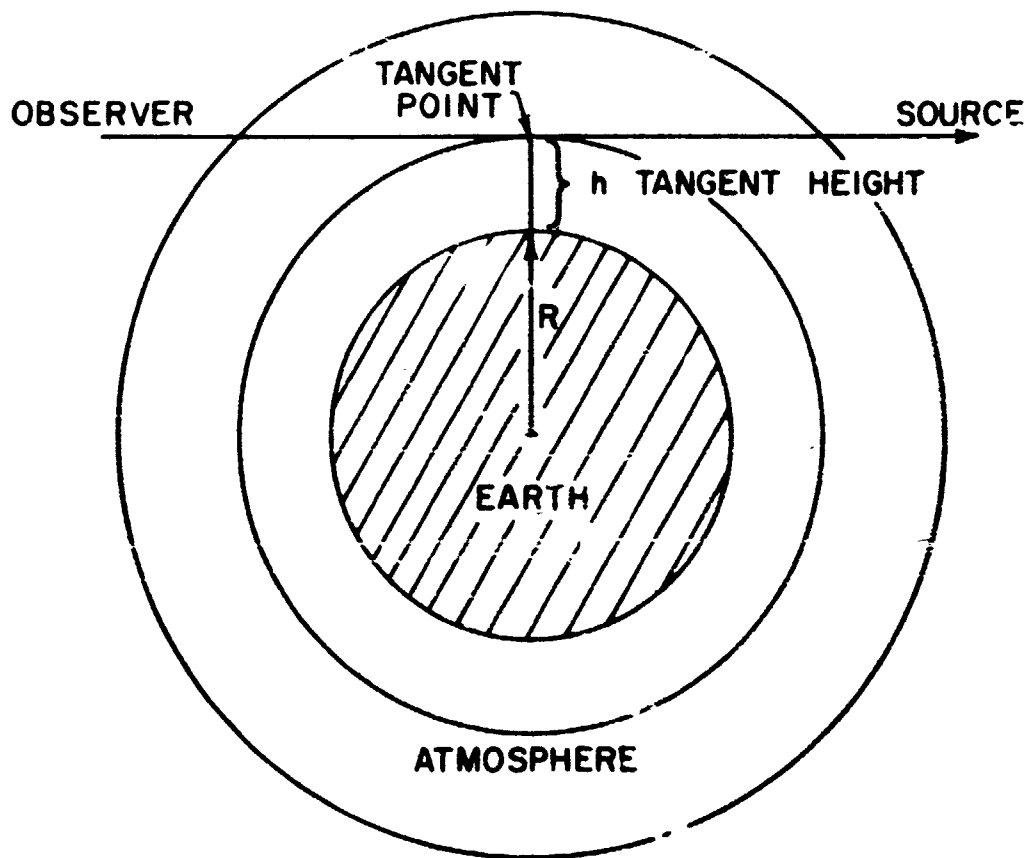


Figure 10: Occultation experiment

Absorption is another quantity which can be measured in occultation since the net effect of the atmosphere on the occultation signal is due to both refractive variations and absorption. In 1966, a Stanford study (Lusignan et al., 1969) showed that the main source of error in the occultation system is water vapor in the lower atmosphere and that using the amplitude of the occultation signals themselves, the absorption due to water vapor could be used to determine the average water content. This effect will be superposed over the effect of refraction. Most of the absorption would take place within a fraction of a scale height of the tangent point since the atmospheric density and pressure fall off exponentially with height. The refractive effects will also occur near the tangent point.

The Stanford group also proposed the use of a passive microwave sensor at 22.235 GHz to monitor the absorption due to water vapor and thus provide for an independent source of absorption data. To date, the use of the passive absorption experiment has had difficulty with vertical resolution (Lusignan et al., 1969).

The occultation technique became an accepted experimental process when the Mariner 4 and 5 spacecraft detected surprising density profiles in the martian atmosphere using a single frequency bistatic radar measurement of the phase path variations. For more detail on the theory see Fjeldbo et al., (1965).

Advantages of this measurement technique are the following: long term measurements can be made (compared to a rocket or aircraft); large areas can be monitored in a short period of time; the outgassing of water vapor is less of a problem after a relative short time. However, equipment packages capable of operating over long periods of time must be obtained.

6.2.2 Active Configurations (resonant absorption)

In this method, the integrated water vapor concentration is measured along a one way path through the atmosphere using the absorption of an active source (a source which requires a separate supply of power to create radiation).

The frequency of the source is first tuned to the center of an absorption line. The intensity of radiation at the detector is then given by

$$I_{on} = I_o T_{air} \exp \left[- \int_0^R K_a N (R) dR \right] \quad (6.6)$$

where

I_o is the intensity of the radiation source

T_{air} is the atmospheric transmission function for dry air

R is the path length

The transmitter is then detuned so that the frequency is outside of the absorption line. The intensity received by the detector is then

$$I_{off} = I_o T_{air} \quad (6.7)$$

The integrated concentration is determined from the ratio between the on and off line intensities and is given by

$$\int_0^R N (R) dR = \frac{1}{K_a} \ln \left[\frac{I_{off}}{I_{on}} \right] \quad (6.8)$$

6.2.2.1 Ground Based Observations
(resonant absorption-active)

In this configuration a ground based radiometer could measure the absorption of radiation from a rocket, balloon, or satellite. However, only the total integrated water vapor density will be known. Thus this observation will suffer from the lack of vertical resolution. The experiment has been performed using a ruby laser emission line at $6943.00 \text{ \AA}^{\circ}$ and tuning the laser cavity in order to shift the line so that it coincides with the $6943.815 \text{ \AA}^{\circ}$ line of water vapor. The measurements have only been made in the lowest few kilometers of the atmosphere, but the method is capable of extension to greater heights.

The advantages of this system are the following: one has control of the source characteristics; noise can be minimized by using narrow bandwidth signals. Most all the other ground based equipment advantages apply here also.

The disadvantages are that the frequency of the transmitter must now be controlled and that radiation has to be produced. This means that permission must be obtained from federal regulatory bodies. Also, the receiver and transmitter have to be in different locations, which can lead to a very expensive experiment.

6.2.2.2 Observations from Above the Surface
(resonant absorption-active)

This configuration could be used between two different spacecraft. For example, a fixed balloon platform at 30 km containing the source and then monitor this source with a radiometer on board a rocket. It may also be used between two rockets or two satellites. The latter is the active occultation experiment and consists of two satellites in orbit which can be spaced so that different line of sight paths can be chosen

between the two. This experiment has great promise for examining quite carefully upper atmospheric layers. The theory of this type of experiment has been discussed in section 6.2.1.3.

Advantages of such systems are the ability to control the source characteristics and that the measurements would be free of the effects of lower atmospheric water vapor. However, the vehicles carry water vapor into the measurement region, thus providing a possible error source. Another problem to be dealt with is the existence of a shock wave which builds up around any supersonically traveling body such as a rocket. This shockwave is a layer of air at a different temperature than the air making up the atmosphere. This difference in temperature gives rise to a difference in refractivity between the antenna and the external atmosphere. As the speed of the body increases, the temperature of the layer increases and at a sufficiently high temperature, the layer becomes a plasma (ionized gas) which can prevent the reception of radio signals.

However, even more important is the fact that two independent vehicles introduce such complexities into the measurement that its feasibility becomes vanishingly small.

6.3 Resonant Emission

6.3.1 Passive Configuration

This method also the least costly, monitors the emission spectra of water vapor from any point in the atmosphere. The equation describing this process for a horizontally stratified atmosphere and a flat earth is (Meeks and Lilley, 1963).

$$T_b = \int_h^{\infty} \sigma(x) T \exp\left[-\int_h^x \sigma(x) \sec \phi dx\right] \sec \phi dx \quad (6.9)$$

where

T_b is the antenna temperature observed by an antenna with an infinitesimally narrow beam

T is the kinetic temperature of the atmosphere

h is the height of the antenna above the earth's surface

ϕ is the angle between zenith and the direction of observation

$\sigma(x)$ is the atmospheric attenuation coefficient at slant range x

This equation describes the emission taking place within the atmosphere along the slant path.

6.3.1.1 Ground Based Observations (resonant emission-passive)

Spectral emission techniques are presently used for the bulk of the microwave atmospheric studies. Those observations near a wavelength of 5 mm (or 60GHz) are dominated by the thermal emission from molecular oxygen. By varying the depth of penetration into the atmosphere, the temperature structure in the lower atmosphere may be determined. Two methods are available for varying the depth of penetration. First, one can make observations at different frequencies at a fixed zenith angle, such that those frequencies least attenuated by absorption features of oxygen will penetrate the atmosphere further. Second, one can make observations at different zenith angles, at a fixed frequency so that at large zenith angles, longer paths through the atmosphere are probed than at smaller zenith angles. As the path length through the atmosphere increases with zenith angle, there is a corresponding increase in attenuation for a plane parallel atmosphere. The path length is proportional to the secant of the zenith angle and if the atmosphere were horizontally stratified

$$\tau(\phi) = \tau_0 \sec \phi \quad (6.10)$$

where

ϕ is the zenith angle and

τ_0 is the vertical atmospheric opacity or optical depth

For the case of the spherical atmosphere, the secant law is useful up to zenith angles of about 85° (Wuifsberg, 1967).

In both of the above methods, it is necessary to have temperature information. Also equation 6.9 must be inverted.

The inversion process is very important to the accuracy of the observational data. Considerations for this process are the following: how does the technique handle noise in the observational data, how fast does the particular technique converge to a solution and is that solution unique and real. The most serious error is imposed by numerical differentiation which grossly amplifies any noise or observational error.

Spectral emission observations at wavelengths near 1.35 cm detect the thermal emission from water vapor and have been shown to be an effective method of inferring crude tropospheric water vapor profiles, integrated water vapor, and stratospheric water vapor. The observations can also differentiate liquid water from water vapor by virtue of the different spectral responses in the two cases. For this purpose, a microwave channel in the 0.8 to 1 cm range of wavelengths where these differences are easily detectable is desirable. Microwave sensors come closer than any other sensor to having all weather capability. Like most passive microwave atmospheric studies, the method may be regarded as still in the stage of infancy and its full potential has not been fully explored. However, since ground based measurements of water vapor

are not sensitive to the atmosphere above 5 km, it is necessary to consider space based observations.

Advantages of this passive system are that there is no need to create radiation and the low cost of an experiment. However, this experiment is not as sensitive to small concentrations as is that of resonant absorption.

6.3.1.2 Observations from Above the Surface (resonant emission-passive)

Detection of water vapor in the upper atmosphere can be accomplished using vehicles in space in the following manner. 1) view the surface of the earth from above in which case the emissivity of the surface viewed must be known, this is discussed further in the text. 2) view the atmosphere along an upward slant path where the emission spectra of the water vapor present along the line of sight path is monitored.

Spaceborne, downward looking experiments at wavelengths near the water vapor resonance line at 1.35 cm are capable of sensing atmospheric water vapor and liquid water content of clouds over oceans. This method is at least an order of magnitude less sensitive over land surfaces. The major reason for the difference in the two cases is that the microwave temperature of the oceans is $\sim 150^{\circ}\text{K}$ because of the low emissivity of water, whereas the microwave temperature of land is $\sim 300^{\circ}\text{K}$. Since the atmospheric water vapor is near 280°K , the contrast between the water vapor and background is considerably enhanced over the oceans. Staelin (1968) reported that this configuration could be used to determine the integrated water vapor content to within about 0.1 gm-cm^{-2} when coupled with a microwave temperature sounding experiment. How-

ever, this temperature sounding experiment will present additional complications in a spaceborne probe.

As was mentioned in section 6.2.1.2, the upward viewing experiment seems very appealing. For this configuration however the radiometer must scan only the cold background atmosphere ($\sim 300^{\circ}\text{K}$) in order to measure the emission spectra. This experiment is less sensitive than the passive absorption measurement. But if sensitivity is not a problem, then the emission experiment could be much easier to perform since it should be much easier to keep the antenna fixed on the cold background than on a hot source of radiation which has a much smaller solid angle. Most of the other advantages and disadvantages which have been discussed in section 6.2.1.2 apply here also.

6.3.2 Active Configuration (resonant emission-active)

In this method also known as resonant scattering, the molecules in a region are excited by the transmitter beam and then the excited molecules emit radiation spontaneously into a solid angle of 4π steradians. Measuring the emitted radiation determines the relative concentration of the molecules.

This emission only occurs when the wavelength of the incident radiation is close to that of an absorption line. Since the cross section will vary across the absorption line and since most experiments performed use radiation with a bandwidth greater than that of the absorption line, it is convenient to discuss an integrated back-scattering function

$$\int_{\Delta\nu} \beta(\nu) d\nu$$

c-2

where $\beta(\nu)$ is the backscattering function at frequency ν . It can be shown that

$$\int_{\Delta\nu} \beta(\nu) d\nu = \frac{e^2 f'_{nn}}{16\pi\epsilon_0 mc} \quad (6.11)$$

where

f'_{nn} is the oscillator strength of the transition (the equivalent number of harmonic oscillators required to yield the same strength) and is given by

$$f'_{nn} = \frac{hm\nu'_{nn}}{\pi e^2} B'_{r'_{nn}} \quad (6.12)$$

e is the charge of an electron

m is the mass of an electron

ϵ_0 is the free space permittivity

c is the speed of light

h is Planck's constant

and

$B'_{r'_{nn}}$ is Einstein's coefficient for induced emission

The value of $B(\nu)$ will depend on the oscillator strength of the transition as well as the line shape, but will be many orders of magnitude greater than the Rayleigh scatter.

6.3.2.1 Ground Based Measurements (resonant emission-active)

This method has been put to use in recent years using high power lasers to excite the medium. At the present, the state of the art (size vs. power) requirements of lasers limit their use to ground based measurements. This mechanism does have one strength which may

make it a very promising technique in the future. Derr et al. (1970) reported that resonant emission is quenched or perturbed and is rarely observed at high atmospheric pressures. This is because resonant emission has characteristic re-emission times of the order of 10^{-8} seconds to 10^{-1} seconds whereas the average time between air molecule collisions in the troposphere is usually very short ($\approx 10^{-9}$ seconds). Fifteen kilometers is, with few exceptions, a lower limit on the observation of resonant emission (Derr et al., 1970).

The method has only been used to detect sodium at very high altitudes thus far, however, there is only a small concentration of sodium. The detection was made possible by the very strong resonant line of sodium. Thus the technique has potential for use in detection of any molecule which has a strong resonant line such as water vapor.

Advantages of this system are that control of the source allows accurate phasing of the source pulse to the receiver and narrow bandwidth signals can be used to limit noise. However, a strong power source is required. This is no problem on the ground, but in space, it is out of the question at the present time.

6.4 Raman Scatter

In this method (always active), a source of fixed frequency is used to excite a volume of molecules which in turn will scatter (reradiate instantaneously) the energy with a shift in frequency characteristic of the molecule.

The return power P_r from the range R is given by (Kobayasi, 1970)

$$P_r = \frac{P_o \eta k T_L T_r A_r Y(R) N(R) \sigma_r (\pi)}{R^2} \quad (6.13)$$

where

- P_o is the transmitted power
 t is one half the pulse length
 k is the total efficiency of the receiver and transmitter
 T_L is the atmosphere transmittance at the transmitter frequency
 T_r is the atmosphere transmittance at the Raman shifted frequency
 A_r is the effective receiver area
 $Y(R)$ is the geometrical factor that accounts for overlap of the transmitter and receiver beam paths
 $N(R)$ is the density of the molecules and
 $\tau_r(\pi)$ is the Raman vibrational-rotational backscattering differential cross-section

The Raman scatter cross-section is inversely proportional to the fourth power of the wavelength, thus the largest cross-section would be in the ultraviolet region of the spectrum. The visible region has the next largest cross-section ($\sim 10^{-28}$ cm²/sr). However, of all the processes considered, this method has the smallest cross-section (the average Raman cross-section is of the order of 4×10^{-3} that of the Rayleigh cross-section for atmospheric gases). This is the main problem with using this method in the microwave region where the cross-section is of the order of 10^{-46} cm²/sr.

6.4.1 Ground Based Observations (Raman scatter-active)

This method has been used for detection of the major atmospheric components such as N₂ and O₂, also for H₂O in the lower atmosphere where the density of H₂O is greatest. This technique has not been used (to the author's knowledge) for observations above the surface (excluding

smokestack observations). This is most likely due to the low sensitivity of the method to the small concentrations of molecules and atoms present in the upper atmosphere. At present the method is limited to ground-based measurements, thus space-based observations will not be considered.

Advantages of Raman scatter are in its ability to avoid completely the ambiguity in the return at the transmitter frequency due to the Mie and Rayleigh scattering components. Moreover, the Raman method requires only a single wavelength source where in general, the resonant absorption and resonant emission schemes require a tunable source.

Disadvantages in addition to the small cross-section are the following: that since all molecules in the atmosphere contribute to the Raman scattering, good filtering techniques are required to select the Raman signal for the constituent of interest; the requirement of high power transmitters; the lack of sensitivity over long distances (Kildal et al., 1971).

CHAPTER VII

SUMMARY AND DISCUSSION

Present knowledge of water vapor concentrations above 30 km is extremely meager. Estimates of volume mixing ratios of 1-3 ppm are widely used, however realistically one cannot rule out uncertainties of plus or minus an order of magnitude about this level. These uncertainties complicate our understanding of fundamental atmospheric processes and structural models. Consequently the significance of an upper atmospheric water vapor measurement is becoming clearer.

The present work is intended to form a comprehensive background for the development of a measurement technique. It deals with the following areas of interest: what is known and presumed of water vapor in the upper atmosphere; the molecular properties of H₂O, especially in the microwave but to a lesser extent in the infrared; radiative transfer and scattering theory as they apply to atmospheric measurement problems; and a survey of measurement configurations.

In the microwave region, water vapor has two rotational lines at about 22.2 GHz (1.35 cm) and 183 GHz (1.64 mm). The 22 GHz line is by far the weaker of the two but lies in a relatively uncluttered region of the spectrum (see Figs. 11 and 12) for which adequate transmitting and receiving equipment is already developed. Millimeter wave instrumentation development could easily make the 183 GHz line rather attractive for the mesospheric measurement where sensitivity is essential. There is a close lying O₃ line, as shown in Fig. 12, however it is at least an order of magnitude weaker.

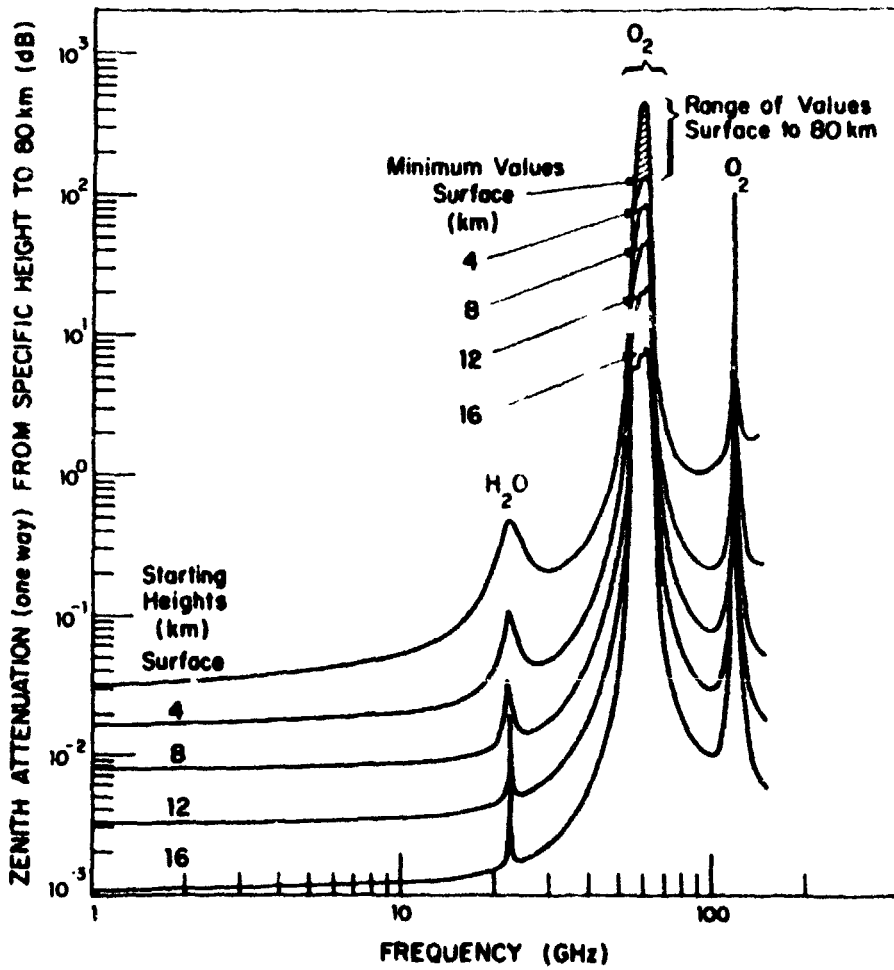


Figure 11: Zenith attenuation versus frequency (Crane, R. K., 1971; reprinted by permission of the Institute of Electrical and Electronic Engineers, Inc.)

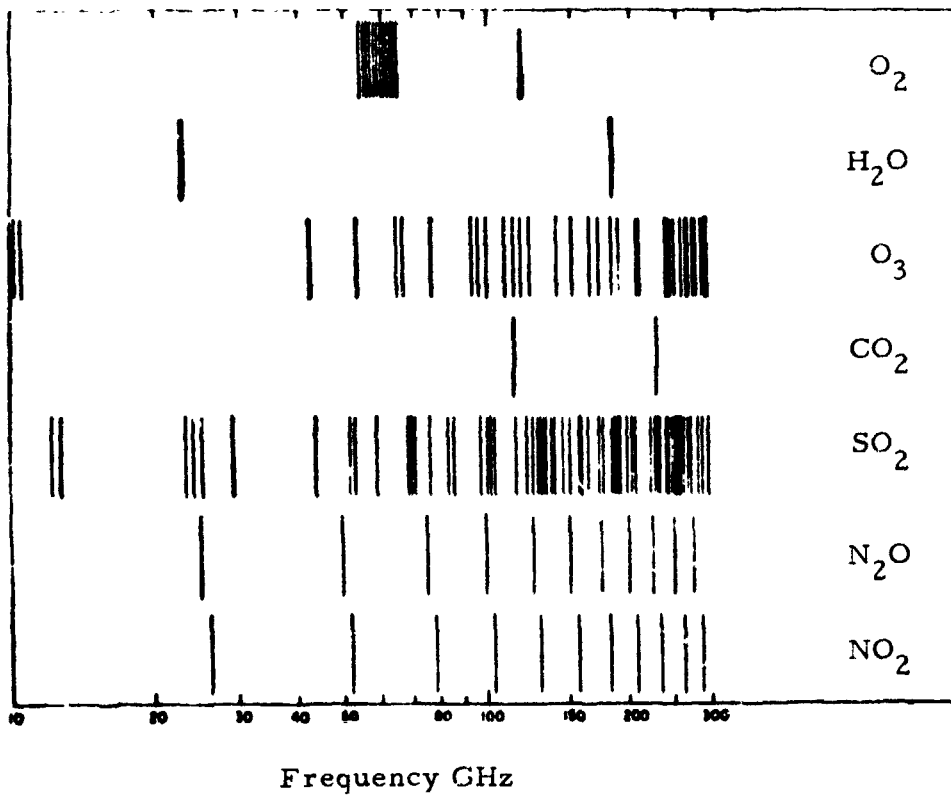


Figure 12: Line frequencies of several atmospheric gases (Tolbert, C. W. et al, 1963; reprinted by permission of the Institute of Electrical and Electronic Engineers, Inc.)

There are a multitude of vibrational-rotational bands of water vapor through the infrared. Among these, strong bands between 1.3μ and 1.9μ and at 6.3μ appear quite attractive and should be looked at in more detail. Tuneable laser technology at these wavelengths is now available promising rather sensitive absorption measurements from active configuration experiments.

The satellite occultation configuration is clearly superior to the others considered. First of all, it alone could provide a truly global water vapor measurement which is necessary for the specific aeronomic and ionospheric problems which bear on the stratospheric and mesospheric water vapor concentrations. Secondly, the large atmospheric paths lengths associated with the occultation configuration appear to be very necessary in view of the low water vapor concentrations likely to be found in the mesosphere. Finally, maximum sensitivity for microwave as well as infrared wavelengths, appears to require an active, two vehicle configuration. The simplest configuration which meets all these criteria involves two vehicles in closely spaced station keeping orbits.

The next step appears to be detailed engineering calculations with specific hardware and orbital vehicles in mind.

APPENDIX A
THE WATER VAPOR MOLECULE

The water vapor molecule (H_2O) is an asymmetric top molecule and has a very complicated spectrum. The dipole moment is very strong (1.85 Debye) and thus the molecule undergoes very strong electric dipole transitions. The molecule has three non-degenerate eigenvibrations, two of which are symmetric and one antisymmetric. All three of its principal moments of inertia are different. The molecule can be represented by a plane model which has the property that the sum of the two principal moments lying in the plane is equal to the moment of inertia perpendicular to the plane. This, however, does not simplify the equations of motion. In the unexcited state, the water vapor molecular configuration has the form of an isosceles triangle with side length $S_{\text{OH}} = 0.958 \text{ \AA}$ (nucleus to nucleus) hydrogen oxygen distance and an apex angle $\theta = 104^\circ 30'$. The absorption of radiation by water vapor in the region from 0.54 to 9μ is caused by vibrational-rotational transitions and in the far-infrared (from 9μ to 1.5 cm) by purely rotational transitions. In the far ultra-violet ($\lambda < 0.2\mu$), the absorption is determined by electronic transitions, dissociation, and ionization.

The rotation-vibration spectrum has been accurately mapped from 135μ to 5700 \AA . Ghosh and Edwards (1956) compiled a listing of H_2O resonance lines in the microwave and far infrared regions. The pure rotational spectrum reaches its maximum intensity around 50μ , from which point it slowly decreases until at about 15μ only a few lines are observable. At about 8.5μ , an intense absorption again sets in, this time due to the outer edge of a fundamental vibration band.

The only significant transitions occurring at frequencies up to 300 GHz are at 22.235 GHz ($J_{\tau}: 5_{-1} \rightarrow 6_{-5}$) and at 183.31 GHz ($J_{\tau}: 2_2 \rightarrow 3_{-2}$).

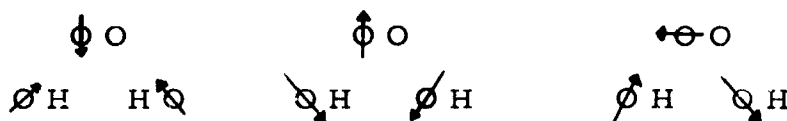
Detailed information on the 22.235 GHz line has been difficult to get with conventional absorption spectroscopy because of the small absorption coefficient ($7.21 \times 10^{-6} \text{ cm}^{-1}$).

Randall et al. (1937) gives a listing of the rotational lines of water vapor which is quite extensive. The selection rules governing the allowed transitions of water vapor are given by Dennison (1931).

The selection rules follow from the wave functions and their symmetry properties which describe the energy levels involved in the transitions. For the electric dipole, the selection rule is $\Delta J = 0, \pm 1$ except $J = 0 \leftrightarrow J = 0$ which is forbidden. For each quantum level J , there are $2J + 1$ nondegenerate energy levels. These energy levels are distinguished by the subscript τ where $\tau = -J$ for the lowest level, $-J + 1$ for the next higher level and so on up to $+J$ the highest level. A transition from one energy state J_{τ} to another J_{τ} of higher energy is accomplished by the absorption of a discrete amount of energy in accordance with the selection rule. $\Delta J > 1$ is forbidden in a dipole transition. The transitions are divided into three branches relating to whether the change in J (ΔJ) is -1 , 0 , or $+1$ and are known as the P, Q, and R branches, respectively. $\Delta J = +1$ corresponds to absorption and $\Delta J = -1$ corresponds to emission thus the P branch does not contribute to the absorption of energy (Hall, 1967).

Each level of the molecule is given a symbol ($++$), ($+ -$), ($- +$), or ($--$) which denotes the symmetry group to which the level belongs. Since in water vapor, the electric moment lies along the middle axis of inertia, the only radiative transitions are those connecting the levels

(++) ↔ (--) or (+-) ↔ (-+). There are three types of normal vibrations of the water vapor molecule which are observed to have the following main wave numbers.



$$\nu_1 = 3670 \text{ cm}^{-1}$$

$$(\lambda_1 = 2.7\mu)$$

$$\nu_2 = 1675 \text{ cm}^{-1}$$

$$(\lambda_2 = 6\mu)$$

$$\nu_3 = 3790 \text{ cm}^{-1}$$

$$(\lambda_3 = 2.64\mu)$$

All of these types are active in absorption.

The rotational water vapor absorption spectrum is associated with rotational energy transitions caused by the molecule rotation around its axes a, b, c, asymmetrically and in a spinlike manner (see figure 13).

Since the selection rules only allow the transitions (++) to combine with (--) and (-+) to combine with (+-), there is no absorption of the non-resonant type since the electric moment matrix of the molecule contains no diagonal elements. Non-resonant absorption would require diagonal matrix elements and thus would demand that (++) combine with (++) which is not allowed.

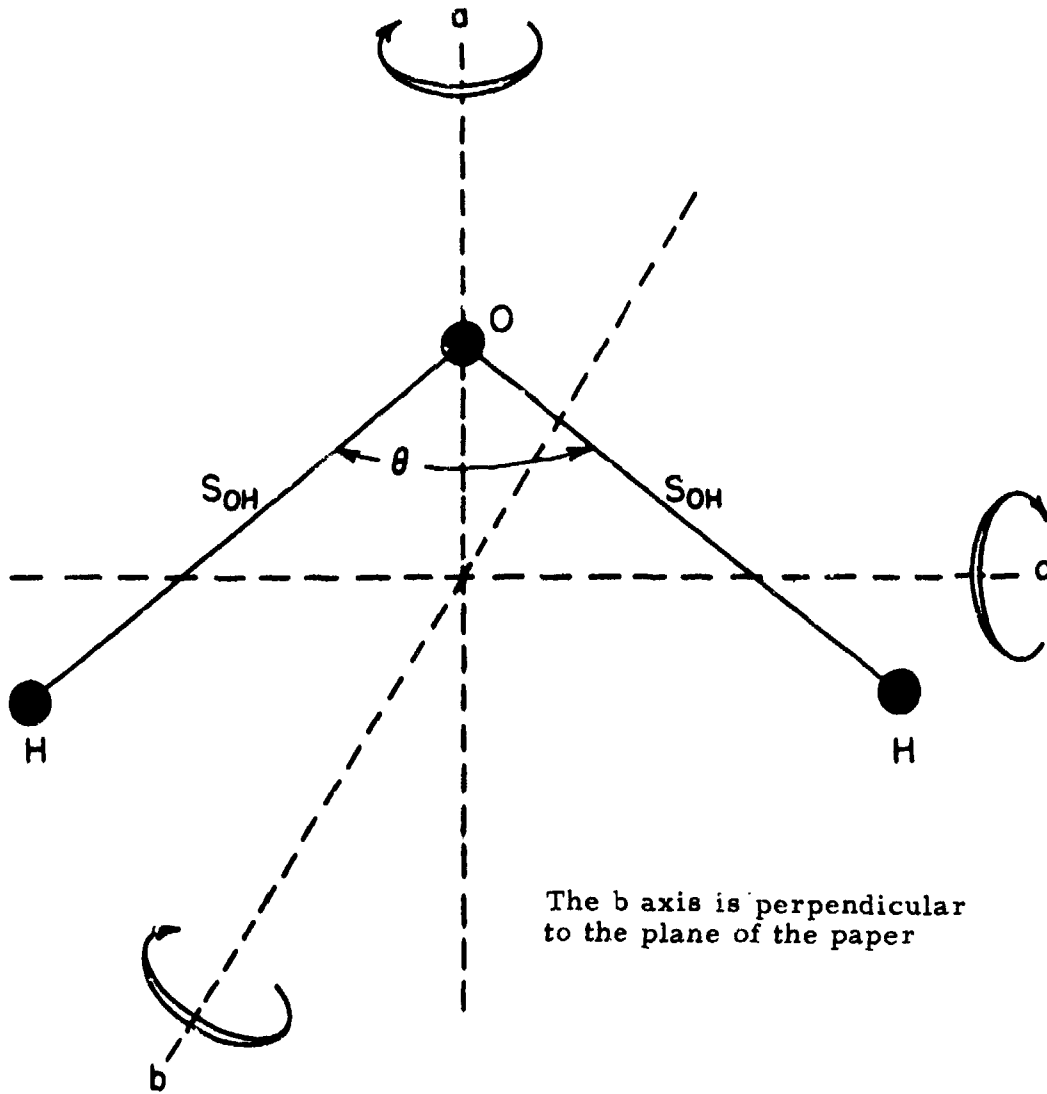


Figure 13: Water vapor molecule

APPENDIX B

MOLECULAR OXYGEN

The oxygen molecule has a number of transitions in the micro-wave region around 60 GHz and a transition at 118.75 GHz. The micro-wave spectrum of the oxygen molecule is a result of fine structure transitions in which the magnetic moment assumes various directions with respect to the rotational angular momentum of the molecule. Oxygen has an intranuclear distance of 1.128 Å. The molecule does not possess an electric dipole moment however it does have a magnetic dipole moment. This magnetic moment arises because the molecule possesses two unpaired electrons. These unpaired spins give a spin quantum number of $S = 1$. The rotational quantum number N (N describes the end over end rotation of the molecule) can only assume odd values because of the exclusion principle.

An odd rotational state N then combines with a spin state to produce a total angular momentum vector with quantum number $J = N - 1$, N , or $N + 1$. Selection rules for the fine structure transitions permit transitions of the form $(J = N) \rightarrow (J = N + 1)$ and $(J = N) \rightarrow (J = N - 1)$. The gyromagnetic ratio $g \frac{e}{2mc}$ has a Lande factor $g = 2$. Thus the oxygen molecule has a magnetic dipole moment of two Bohr magnetons. This magnetic moment interacting with the magnetic field of the micro-wave radiation results in absorption of energy. At high altitudes, the Zeeman effect in oxygen cannot be neglected. The earth's magnetic field will split the oxygen lines into separate components. Each quantum state of the molecule specified by the quantum number J will be split into $2J + 1$ magnetic substates. The fine structure transitions $\Delta J = \pm 1$

proceed according to the selection rules $\Delta M = 0, \pm 1$ where M is the magnetic quantum number. Generally there are $3(2J' + 1)$ Zeeman components in the transition where J' is the smaller of the two J values involved. In the case of oxygen, there is non-resonant absorption since the absorption is caused by the magnetic dipole moment for which the rule is that + combines with + and - combines with -. This gives rise to the matrix for the magnetic dipole moment having diagonal matrix elements.

APPENDIX C

MIE SCATTER APPROXIMATION

Penndorf (1962) has obtained an approximation formula which will extend the Rayleigh range by about a factor of 2. This formula can be derived from Mie's formula using the series expansion method. For real indices of refraction n , the total scattering coefficient is

$$K_s^{\text{mie}} = \frac{8\alpha_1^4}{3} \left(\frac{n^2 - 1}{n^2 + 2} \right)^2 \left[1 + \frac{6\alpha_1^2}{5} \left(\frac{n^2 - 2}{n^2 + 2} \right) + \alpha_1^4 A \right] \quad (\text{C. 1})$$

where

$$A = \frac{3}{175} \left(\frac{n^6 + 41n^4 - 284n^2 + 284}{(n^2 + 2)^2} \right) + \frac{1}{900} \left(\frac{n^2 + 2}{2n^2 + 3} \right)^2 \left[15 + (2n^2 + 3)^2 \right] \quad (\text{C. 2})$$

and $\alpha_1 = \frac{2\pi a}{\lambda}$, the size parameter. Note that the first term is the Rayleigh formula

$$K_s = \frac{128\pi^4 a^4}{3\lambda^4} \left(\frac{n^2 - 1}{n^2 + 2} \right)^2 \quad (\text{C. 3})$$

This approximation (C. 1) can be used up to a size parameter of $\alpha_1 = 1.4$ and $n < 2$. The error between the exact computation (Mie) and K_s will remain below 2 percent up to $n = 1.5$ and reach 15 percent at $n = 2$.

For the case where the indices of refraction are complex ($m = n - i\chi$), the total extinction coefficient is

$$K_s^{\text{Ext}} = \frac{24n\chi}{Z_1} \alpha_1 + \alpha_1^3 \left[\frac{4n\chi}{15} + \frac{20n\chi}{3Z_2} \right]$$

$$+ 4.8n\chi \left[\frac{7(n^2 + \chi^2)^2 + 4(n^2 - \chi^2 - 5)}{Z_1^2} \right] \quad (C.4)$$

$$+ \frac{8\alpha_1^4}{3} \left[\frac{([n^2 + \chi^2]^2 + [n^2 - \chi^2 - 2]^2) - 36n^2\chi^2}{Z_1^2} \right]$$

where

$$Z_1 = (n^2 + \chi^2)^2 + 4(n^2 - \chi^2) + 4 \quad (C.5)$$

$$Z_2 = 4(n^2 + \chi^2)^2 + 12(n^2 - \chi^2) + 9$$

The total scattering coefficient is

$$K_s^{Mie} = \frac{8B\alpha_1^4}{3Z_1^2} \left[\left((n^2 + \chi^2)^2 + n^2 - \chi^2 - 2 \right)^2 + 36n^2\chi^2 \right] \quad (C.6)$$

where

$$B = 1 + \frac{6}{5Z_1} \left([n^2 + \chi^2]^2 - 4 \right) \alpha_1^2 - \frac{24n\chi}{3Z_1} \alpha_1^3 \quad (C.7)$$

These two equations (C.4), (C.6) lead to reliable values for $\alpha_1 \approx 0.8$ in the range $n = 1.25$ to $n = 1.75$ and $\chi \leq 1$. For any larger particle the exact Mie formulas have to be used. The useful size range for water droplets at weather radar frequencies for which complex indices of refraction pertain, is restricted to about $\alpha_1 \leq 0.2$.

APPENDIX D

DERIVATION OF ELSASSER'S INFRARED ABSORPTION MODEL

From section 5.2 the fractional absorption for the entire band is

$$A = \frac{1}{2\pi} \int_{-\pi}^{\pi} 1 - \exp(-K_a W) dx \quad (D.1)$$

From the definition in section 5.2

$$K_a W = \frac{S_o W \pi \Delta \nu}{d^2 \sin^2 x/2} = \frac{\alpha^2}{\sin^2 x/2} \quad (D.2)$$

where

$$\alpha \equiv \frac{\sqrt{S_o W \pi \Delta \nu}}{d} \quad (D.3)$$

if we let

$$u = \frac{\alpha}{\sin x/2} \quad (D.4)$$

The integral can be written

$$A = 1 - \frac{2\alpha}{\pi} \int_{\alpha}^{\infty} \frac{e^{-u^2}}{u \sqrt{u^2 - \alpha^2}} du \quad (D.5)$$

The integral then may be transformed into

$$A = 1 - \frac{2\alpha}{\pi} e^{-\alpha^2} \int_0^{\infty} \frac{e^{-z^2}}{z^2 + \alpha^2} dz \quad (D.6)$$

through the substitution

$$Z = \sqrt{u^2 - a^2} \tag{D.7}$$

To evaluate this integral, let

$$I(a) = \int_0^{\infty} \frac{e^{-a^2 x^2}}{x^2 + a^2} dx \tag{D.8}$$

then

$$\begin{aligned} I'(a) &= -2a \int_0^{\infty} e^{-a^2 x^2} dx + 2a a^2 \int_0^{\infty} \frac{e^{-a^2 x^2} dx}{x^2 + a^2} \\ &= -\sqrt{\pi} + 2a a^2 I(a) \end{aligned} \tag{D.9}$$

or

$$\frac{dI}{da} - 2a a^2 I = -\sqrt{\pi} \tag{D.10}$$

which has the solution

$$I e^{-a^2 a^2} = -\sqrt{\pi} \int_0^a e^{-t^2 a^2} dt + c \tag{D.11}$$

Then from (D.8)

$$I(0) = \int_0^{\infty} \frac{dx}{x^2 + a^2} = \frac{1}{a} \operatorname{Tan}^{-1} \left(\frac{x}{a} \right) \Big|_0^{\infty} = \frac{\pi}{2a} \tag{D.12}$$

which implies that $C = \frac{\pi}{2\alpha}$, thus

$$\begin{aligned}
 I(a) &= \frac{\pi}{2\alpha} e^{a^2 \alpha^2} - \frac{\pi}{2\alpha} e^{a^2 \alpha^2} \frac{2}{\sqrt{\pi}} \int_0^{a\alpha} e^{-u^2} du \\
 &= \frac{\pi}{2\alpha} e^{a^2 \alpha^2} \left[1 - \operatorname{erf}(a\alpha) \right]
 \end{aligned}
 \tag{D.13}$$

where

$$\operatorname{erf}(a\alpha) \equiv \frac{2}{\sqrt{\pi}} \int_0^{a\alpha} e^{-u^2} du
 \tag{D.14}$$

For the integral in equation (D.6)

$a = 1$ and the result is

$$A = \operatorname{erf}(\alpha) \text{ where}
 \tag{D.15}$$

$$\alpha \equiv \frac{\sqrt{S_0 W \pi \Delta \nu}}{d}
 \tag{D.3}$$

REFERENCES

- Altshuler E. E. et al, "Atmospheric Effects on Propagation at Millimeter Wavelengths." IEEE Spectrum, 5, pp. 83-90, July 1968.
- Anderson, A., "The Raman Effect," Marcel Dekker, Inc., New York, 1971.
- Anderson, J. G., "Rocket-borne Ultraviolet Spectrometer Measurement of OH Resonance Fluorescence with a Diffusive Transport Model for Mesospheric Photochemistry," J. Geophys. Res., 76, pp. 4634-4652, 1971.
- Barrett, A. H., "Spectral Lines in Radio Astronomy," Proceedings of the IEEE, 46, pp. 250-259, 1958.
- Barrett, A. H. and Chung, V. K., "A Method for the Determination of High Altitude Water Vapor Abundance from Ground Based Microwave Observations," J. Geophys. Res., 67, pp. 4259-4266, 1962.
- Bean, B. R., "The Radio Refractive Index of Air," Proceedings of the IRE, 50, pp. 260-273, 1962.
- Benedict, W. S. and Kaplan L. D., "Calculations of Line Widths in H₂O - N₂ Collisions," J. Chem. Phys., 30, pp. 388-399, 1959.
- Benedict, W. S. et al, "Calculation of Line Widths in H₂O - H₂O and H₂O - O₂ Collisions," J. Quant. Spectrosc. Radiat. Transfer 4, pp. 453-469, 1964.
- Becker, G. E. and Autler, L. H., "Water Vapor Absorption of Electromagnetic Radiation in the Centimeter Wave Length Range," Phys. Rev., 70, pp. 300-307, 1946.

- Bonvini, L. A. et al, "A Search for the 22.235 GHz Emission Line from Stratospheric Water Vapor," J. Atmos. Terrest. Phys., 28, pp. 891-896, 1966.
- Bowman, M. R. et al, "The Effect of Diffusion Processes on the Hydrogen and Oxygen Constituents in the Mesosphere and Lower Thermosphere," J. Atmos. Terrest. Phys., 32, pp. 1661-1674, 1970.
- Bradford, et al, "Absolute Solar Spectra 3.5-5.5 Microns, Theoretical Spectra for Altitude Range 15-30 km," Applied Optics, 3, pp. 459-465, 1964.
- Collis, R. T. H., "Lidar", Atmospheric Exploration by Remote Probes Proceedings of the Scientific Meetings of the Panel on Remote Atmospheric Probing, 2, pp. 147-173, 1968.
- Cooney, J., "Remote Measurements of Atmospheric Water Vapor Profiles Using the Raman Component of Laser Backscatter," J. App. Meteor., 9, pp. 182-184, 1970.
- Cowling, T. G., Phil. Mag., 41, p. 109, 1950.
- Crane, R. K., "Propagation Phenomena Affecting Satellite Communication Systems Operating in the Centimeter and Millimeter Wavelength Bands," Proceedings of the IEEE, 59, pp. 173-188, 1971.
- Croom, D. L., "The Possible Detection of Atmospheric Water Vapor from a Satellite by Observations of the 13.5 mm and 1.64 mm H₂O Lines," J. Atmos. Terrest. Phys., 28, pp. 323-326, 1966.
- Croom, D. L., "Stratospheric Thermal Emission and Absorption Near the 183.311 Gc/S (1.64 mm) Rotational Line of Water Vapor," J Atmos. Terrest. Phys., 27, pp. 235-243, 1965.

- Croom, D. L., "Stratospheric Thermal Emission and Absorption Near the 22.235 Gc/s (1.35 cm) Rotational Line of Water Vapor," J. Atmos. Terrest. Phys., 27, pp. 217-233, 1965.
- Debye, P., "Polar Molecules," The Chemical Catalog Company, Inc., 1929.
- Dennison, D. M., "The Infrared Spectra of Polyatomic Molecules (Part I)," Rev. Mod. Phys., 3, pp. 280-345, 1931.
- Dennison, D. M., "The Infrared Spectra of Polyatomic Molecules (Part II)," Rev. Mod. Phys., 12, pp. 175-214, 1940.
- Derr, V. E. and Little, C. G., "A Comparison of Remote Sensing of the Clear Atmosphere by Optical, Radio, and Acoustic Radar Techniques," Applied Optics, 9, pp. 1976-1992, 1970.
- Dicke, R. H. et al, "Atmospheric Absorption Measurements with a Microwave Radiometer," Phys. Rev., 70, pp. 340-348, 1946.
- Elsasser, W. M., Phys. Rev., 54, p. 126, 1938.
- Fjeldbo, G. and Eshleman, V. R., "The Bistatic Radar-Occultation Method for the Study of Planetary Atmospheres," J. Geophys. Res., 70, pp. 3217-3225, 1965.
- Foley, H. M., "The Pressure Broadening of Spectral Lines," Phys. Rev., 69, pp. 616-628, 1946.
- French, I. P., "Microwave and Far Infrared Absorption as a Diagnostic for the Wake of Hypersonic Projectiles," J. Quant. Spectrosc. Radiat. Transfer, 8, pp. 1655-1673, 1968.
- Ghosh, S. N. and Edwards, H. D., "Rotation Frequencies and Absorption Coefficients of Atmospheric Gas," Geophys. Res. Directorate, A. F. Cambridge Res. Ctr., Bedford, Massachusetts, Report No. 82, 1956.

- Goff, J. A. and Gratch, S., "Low Pressure Properties of Water"
Trans. Amer. Soc. Heating and Ventilating Engineers, 52
pp. 95-115, 1946.
- Goody, R. M., Quart J. Roy. Meteorol. Soc., 78, p. 165, 1952.
- Gross, E. P., "Shape of Collision Broadened Spectral Lines" Phys. Rev.,
97, pp. 395-403, 1955.
- Hajovsky, R. G. and LaGrone, A. H., "The Effects of Aerosols in the
Atmosphere on the Propagation of Microwave Signals,"
J. Atmos. Terrest. Phys., 28, pp. 361-371, 1966.
- Hall, J. T., "Attenuation of Millimeter Wavelength Radiation by Gaseous
Water," Applied Optics, 6, pp. 1391-1398, 1967.
- Herzberg, G., "Infrared and Raman Spectra," D. Van Nostrand Co,
Inc. New York, 1945.
- Howard, J. N. et al, "Infrared Transmission of Synthetic Atmospheres,"
J. Optical Soc. of America, 46, pp. 334-338, 1956.
- Jenkins, F. A. and White, H. E., "Fundamentals of Optics,"
McGraw-Hill Book Co, Inc., New York, 1957.
- Keneshea, T. J. et al, "The Latitudinal Variation of Major and
Minor Neutral Species in the Upper Atmosphere," Space
Research XII, pp. 695-709.
- Kent, G. S. and Wright, R. W. H., "A Review of Laser Radar
Measurements of Atmospheric Properties," J. Atmos. Terrest.
Phys., 32, pp. 917-943, 1970.
- Kildal, H. and Byer, R. L., "Comparison of Laser Methods for the
Remote Detection of Atmospheric Pollutants," Proceedings of the IEEE,
59, pp. 1644-1663, 1971.

- King, G. W. et al, "Expected Microwave Absorption Coefficients of Water and Related Molecules," Phys. Rev., 71, pp. 433-443, 1947.
- Kobayasi, T. et al, "Laser-Raman Radar for Air Pollution Probe," Proceedings of the IEEE, 58, pp. 1568-1571, 1970
- Kondratyev, K. Ya., "Radiation in the Atmosphere," Academic Press, New York, 1969.
- Lusignan, B. et al, "Sensing the Earth's Atmosphere with Occultation Satellites," Proceedings of the IEEE, 57, pp. 458-467, 1969.
- Mastenbrook, H. J., "The Variability of Water Vapor in the Stratosphere," J. Atmos. Sci., 28, pp. 1495-1501, 1971.
- Mastenbrook, H. J., "Water Vapor Distribution in the Stratosphere and High Troposphere," J. Atmos. Sci., 25, pp. 299-311, 1968.
- Meeks, M. L. and Lilley, A. E., "The Microwave Spectrum of Oxygen in the Earth's Atmosphere," J. Geophys. Res., 68, pp. 1683-1703, 1963.
- Meyer, J. W., "Radar Astronomy at Millimeter and Submillimeter Wavelengths," Proceedings of the IEEE, 54, pp. 484-492, 1966.
- Penndorf, R., "Scattering and Extinction Coefficients for Small Spherical Aerosols," J. Atmos. Sci., 19, p. 193, 1962.
- Plass, G. N., J. Opt. Soc. Am., 48, p. 690, 1958.
- Plass, G. N., J. Opt. Soc. Am., 50, p. 868, 1960.
- Randall, H. M. et al, "The Far Infrared Spectrum of Water Vapor," Phys. Rev., 52, pp. 160-174, 1937.
- Rosenblum, E. S., "Atmospheric Absorption of 10-400 GHz Radiation," The Microwave Journal, 4, pp. 91-96, 1961.

- Schulze, A. E. and Tolbert, C. W., "Shape, Intensity, and Pressure Broadening of the 2.53 Millimeter Wavelength Oxygen Absorption Line," Nature, 200, pp. 747-750, 1963.
- Shimabukuro, F. I., "Propagation Through the Atmosphere at a Wavelength of 3.3 mm," IEEE Transactions on Antennas and Propagation, AP14, pp. 228-235, 1966.
- Shimazaki, T. and Laird, A. R., "A Model Calculation of the Diurnal Variation in Minor Neutral Constituents in the Mesosphere and Lower Thermosphere Including Transport Effects," J. Geophys. Res., 75, p. 3221, 1970.
- Sissenwine, N. et al, "Mid-Latitude Humidity to 32 km," J. Atmos. Sci., 25, pp. 1129-1140, 1968.
- Staelin, D. H., "Passive Remote Sensing at Microwave Wavelengths," Proceedings of the IEEE, 57, pp. 427-439, 1969.
- Straiton, A. W. and Tolbert, C. W., "Anomalies in the Absorption of Radio Waves by Atmospheric Gases," Proceedings of the IRE, 48, pp. 898-903, 1960.
- Tank, W. G., "An On-Board Technique for Estimating the Effect of Water Vapor in Radio Occultation Measurements of Atmospheric Density," J. Geophys. Res., 74, pp. 4147-4156, 1969.
- Tolbert, C. W. and Straiton, A. W., "Synopsis of Attenuation and Emission Investigations of 58 to 62 kmc Frequencies in the Earth's Atmosphere," Proceedings of the IEEE, 51, pp. 1754-1760, 1963.
- Townes, C. H. and Schawlow, A. L., "Microwave Spectroscopy," McGraw-Hill Book Co., New York, 1955.

- Van Vleck, J. H., "The Absorption of Microwaves by Oxygen,"
Phys. Rev., 71, pp. 413-424, 1947.
- Van Vleck, J. H., "The Absorption of Microwaves by Condensed
Water Vapor, Phys. Rev., 71, pp. 425-433, 1947.
- Van Vleck, J. H. and Weisskopf, V. F., "On the Shape of Collision
Broadened Lines," Rev. Mod. Phys., 17, pp. 227-236, 1945.
- Welch, W. J., "A Selective Review of Ground Based Passive Micro-
wave Radiometric Probing of the Atmosphere," Proceedings of
the Scientific Meetings of the Panel on Remote Atmospheric
Probing, 2, pp. 369-396, 1968.
- Westwater, E. R. et al, "Ground Based Microwave Probing,"
Proceedings of the Scientific Meetings of the Panel on Remote
Atmospheric Probing, 2, pp. 397-408, 1968.
- Wulfsberg, K. N., "Atmospheric Attenuation at Millimeter Wavelengths,"
Radio Science, 2, pp. 319-324, 1967.